

EPSC2018

OPS4 abstracts

Juno and the New Renaissance

by Theo Clarke

There is an intangible societal need to connect with the universe. This is why the space program is so popular. Through the space program the people of the world can touch the universe, touch infinity.

Spacecraft reconnaissance of our solar system continues a legacy of exploration ingrained in our psyches. As a human race, we explore. We ask, Who am I and where do I come from? In the process of this exploration the aura and soul of NASA's Juno mission to the planet Jupiter, like the Medici of the Renaissance, has inspired, facilitated and embodied a broad spectrum of human creativity, including not only science and technology, but also history and literature, art and music, and visualization and public engagement. Indeed, through Juno the world is witness to a remarkable convergence of art and science, witness to a New Renaissance. Juno is an ambassador to the universe of this New Renaissance.

In my paper I will unveil the Juno mission at Jupiter, the Earth encounter that slung it to Jupiter, and the amazing cultural connection that defines its mission. I will speak of Juno's public engagement program called Science in a Fishbowl. The Science in a Fishbowl program encourages public participation in processing, in often artistic ways, imaging data taken of Jupiter by JunoCam, the camera on Juno. I will show some of the best of these citizen scientist works of art. I will also assemble and describe a 3-D scale model of the orbital mission of Juno at Jupiter. The scale of the model is $1'' = 2 R_J$.

In summary, I will unveil a dimension of the Juno mission to the planet Jupiter that will appeal to a broad sector of the global public.

Jupiter's 2018 South Temperate Belt Disturbance: Observations and numerical modelling

P. Iñurrigarro (1), R. Hueso (1), A. Sánchez-Lavega (1), J. Legarreta (1) and J. M. Gómez-Forrellad (2)

(1) Escuela de Ingeniería de Bilbao, UPV/EHU, Bilbao, Spain (2) Fundació Observatori Esteve Duran, Barcelona, Spain.
(peio.inurrigarro@ehu.eus)

Abstract

Jupiter's atmosphere exhibits a wide variety of atmospheric phenomena that are investigated by ground-based and spacecraft observations. The Juno mission around the planet observes the planet from close-in in perijoves separated by 53 days. The mission has attracted a strong observational support from amateur astronomers through an organized collaboration with the JunoCam instrument and also from large telescopes including observations by the Hubble Space Telescope scheduled close to many of the Juno perijoves. Convective storms in Jupiter develop frequently at different latitudes, with different intensities and trigger important changes in the planet. In February 2018 a series of convective storms erupted in the South Temperate Belt (STB), inside an elongated cyclonic region of low contrast known as the STB "Ghost", close to oval BA. The interaction between the storms and the cyclone resulted in the development of intense turbulence initially confined to the cyclonic region. Here we report an analysis of observations of this activity from amateur, JunoCam and public HST observations combined with detailed numerical simulations of the event. The event resulted in a complex evolution of the pre-existing ghost and altered oval BA. Our modelling constrains the vertical characteristics of the cyclone and the amount of energy released in the storms.

1. Dynamical context

After being in an overall calm state throughout most of 2016 [1], Jupiter's atmosphere started to display convective activity at different latitudes. In October 2016 four convective storms in Jupiter's North Temperate Belt (NTB) ended up developing a planetary scale disturbance that lasted months [2]. In December 2016 a convective storm in the South Equatorial Belt (SEB) developed also a large-scale

disturbance in this region with large-scale turbulence extending over several months. In October 2017 a disturbance in the South Tropical Zone observed by several telescopes and the JunoCam instrument on Juno developed a South Tropical Zone Disturbance with a recirculation of the zonal winds followed by its interaction with the Great Red Spot over 2018. In February 2018 a series of convective storms erupted in a matter of 3 days in the South Temperate Belt (STB) inside a low-contrast elongated cyclonic region (the so-called STB Ghost) developing strong turbulence initially confined to the cyclonic Ghost developing a South Temperate Belt Disturbance (STBD).

2. Amateur observations

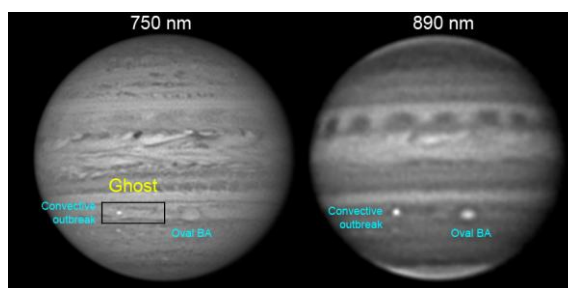


Figure 1: Convective outbreak in the STB Ghost.
Observations by A. Wesley on 4 February 2018.

The onset of convection was discovered on observations obtained by different amateur astronomers on February 4, 2018 including observations in the strong methane absorption band demonstrating the convective nature of the bright spot (figure 1). We have followed the later evolution of this event from amateur observations available on the databases: PVOL (<http://pvol2.ehu.eus/pvol2/>) and ALPO-Japan (<http://alpo-j.asahikawa-med.ac.jp/indexE.htm>). The convection left the whole region perturbed with bright and dark filaments. Before the convective eruption the ghost

was drifting in longitude in Jupiter's STB with a drift rate of 0.26 deg/day. By the date of the convective eruption the ghost was at a distance of 17 deg from the large anticyclone BA. The interaction of the East side of the ghost with BA modified their longitudinal drift. The perturbed ghost evolved to break-up on April 1 and produced several anticyclones that were expelled from the cyclonic system through its southwest side. Both ground-based observations and HST show that the close interaction between the STB Ghost and oval BA resulted in a diminishing size of oval BA at an average rate of 0.02 deg/day between February and April 2018.

3. JunoCam and HST observations

We used JunoCam and HST [3] observations of the Ghost feature obtained over 2017 to investigate its nature before the onset of the perturbation. The JunoCam images showed the structure of the ghost but the small time separation between the images resulted in a ghost circulation of 80 ± 20 m/s. Wind measurements over 2017 HST images showed that the cyclone is an elongated feature with a size of $28,000 \times 4,500$ km with an external cyclonic circulation (clockwise) of 60 ± 10 m/s. HST observations on April 17, 2018 showed the broken perturbed system and its interaction with oval BA (Figure 2).

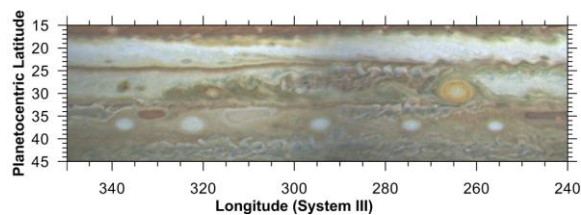


Figure 2: Map of the STB Disturbance and oval BA based on HST observation on April 17, 2018.

4. Simulations

We used the Explicit Planetary Isentropic-Coordinate Atmospheric Model (EPIC) model [4] to investigate the complex interaction between the ghost, the convective outbreaks and the anticyclone BA. We created a numerical “ghost” with the same size, circulation and drift rate as the observations and introduced oval BA. We later perturbed the “ghost” with discrete heat impulses at the location of the convective events following the methodology on [5],

and simulate the interaction of the systems. Figure 3 shows an example of one of these simulations.

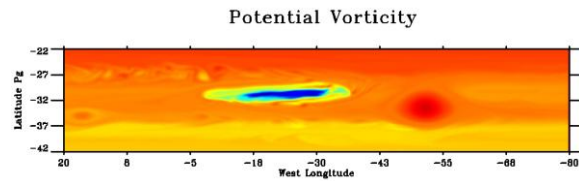


Figure 3: EPIC Simulation of the elongated cyclonic ghost (blue) and the anticyclone BA (red).

5. Summary and Conclusions

Time-resolved observations obtained by amateur astronomers allowed to characterize the evolution of this complex system observing the formation of new ovals expelled from the system. We explored the space of parameters of the modelled atmosphere, STB Ghost vertical structure and intensity of the convective eruptions strongly constraining the dynamics of this complex system.

Acknowledgements

We are very grateful to amateur astronomers posting their observations in image databases like PVOL and ALPO-Japan. This work has been supported by the Spanish MINECO project AYA2015-65041-P with FEDER, UE support and Grupos Gobierno Vasco IT-765-13. P. I. also acknowledges a PhD scholarship from Gobierno Vasco.

References

- [1] Hueso et al.: Jupiter cloud morphology and zonal winds from ground-based observations before and during Juno's first perijove, *Geophys. Res. Lett.*, 44, 4669-4678, 2017.
- [2] Sánchez-Lavega et al.: A planetary-scale disturbance in the most intense Jovian atmospheric jet from JunoCam and ground-based observations, *Geophys. Res. Lett.*, 44, 4679-4686, 2017.
- [3] Simon et al.: First Results from the Hubble OPAL Program: Jupiter in 2015, *ApJ*, 812, id55, 8, 2015.
- [4] Dowling et al.: The Explicit Planetary Isentropic-Coordinate (EPIC) Atmospheric Model, *Icarus*, 132, 221-238, 1998.
- [5] Sánchez-Lavega et al.: Deep winds beneath Saturn's upper clouds from a seasonal long-lived planetary-scale storm, *Nature*, 475, 71-74, 2011.

Jupiter's Evolution with Primordial Composition Gradients

Ravit Helled (1), Allona Vazan (2) and Tristan Guillot (3)

(1) Institute of Computational Science, Center for Theoretical Astrophysics & Cosmology, Switzerland (rhelled@physik.uzh.ch) (2) University of Amsterdam, Anton Pannekoek Institute of Astronomy, Amsterdam, The Netherlands (3) Observatoire de la Côte d'Azur, Bd de l'Observatoire, Nice, France

Abstract

Recent formation models of Jupiter suggest that it could form with composition gradients. This possibility directly affects our understanding of Jupiter's bulk composition and origin.

We present Jupiter's evolution with a primordial structure consisting of a composition gradient with $40 M_{\oplus}$ of heavy elements throughout the planet. We show that for this primordial structure most of the mixing occurs in the outer part of the gradient during the early evolution (several 10^7 yr), leading to an adiabatic outer envelope (60% of Jupiter's mass). We find that in that case the composition gradient in the deep interior persists; suggesting that $\sim 40\%$ of Jupiter's mass can be non-adiabatic (and therefore, not fully-convective) with higher temperatures than the ones derived from adiabatic interiors.

The derived current-state structure can be viewed as Jupiter with a diluted core, as suggested by recent Jupiter structure models that fit *Juno*'s gravity data.

CYCLONIC ACTIVITIES ON JUPITER AND EARTH; CATASTROPHIC ATMOSPHERIC PHENOMENA OF THE WAVE NATURE: EL-NINO, CYCLON, TORNADO

G. Kochemasov; IGEM of the Russian Academy of Sciences, 35 Staromonetny, 119017 Moscow, RF, kochem.36@mail.ru

Atmosphere is one of the outer geographical envelopes occurring under influence of the tectonics of the solid Earth. In its structure is the first order feature – global tectonic dichotomy made by the fundamental wave long $2\pi R$ (Fig. 1) The uplifted continental hemisphere opposes to the subsided Pacific one. This global structure is complicated by superimposed sectors due to the first overtone wave₂ (long πR). Corresponding to the Earth's orbit tectonic granulation has size $\pi R/4$ due to the wave $\pi R/2$. Characteristic tectonic formation of this size (~5000 km in diameter) is a Precambrian platform or a craton with its folded frame. Eight such granules are placed in the great planetary ring – equator (Fig. 3).

To the tectonic dichotomy in the atmosphere correspond two global cells: one with the lower pressure with a centre of constant measurements in Darwin (Australia) on the continental hemisphere and the second with the higher pressure with a centre in the Easter Island in the Pacific hemisphere (Fig. 1, [2]). From the point of view keeping the angular momentum such opposition of atmospheric pressures is understandable: to the uplifting eastern hemisphere with increased radius corresponds the lower pressure, to the subsided oceanic western hemisphere with diminished radius corresponds the higher pressure. Periodic changes of this stable configuration of pressures- increasing pressure in Darwin and lowering over Easter Island – leads to a change of oceanic current in the Pacific, increasing water temperature and origin of unfavorable often catastrophic conditions in the environment.

Cyclones or typhoons with diameters up to several thousands km – cells of the lower pressure – arise normally in the tropics (Fig. 3). Their sizes are typically rather smaller than calculated for tectonic granules (5000 km). One might explain this by a tendency of diminishing sizes of objects in the tropical and equatorial belts for the purpose of diminishing their angular momentum. This process of diminishing is characteristic also for other geospheres. For example, in the lithosphere (crust) there is subsidence of platform bases, in the anthroposphere there is a global phenomenon of pygmeoidness. According to the Le to Chatelier principle, diminishing sizes of atmospheric cells (granules) are compensated by increasing speed of their rotation for keeping their angular momentum. Such rapidly rotating objects, and also taking in moisture for increasing their mass, come down to coasts and inlands with downpours and hurricanes.

Tornado – smaller rotating objects possess huge destructive force (Fig. 2). Their sizes are connected with atmospheric cells made by rotating atmosphere. Under rotating frequency 1/1 day their theoretical size is $\pi R/1460$ or ~14 km in diameter. In fact their size is smaller, reaches about 8 km. This decrease also can be connected with their occurrence in the tropical zones with increased radius demanding decrease of sizes and masses of objects for decreasing the angular momentum. A consequence of this is increase of rotating speed with catastrophic results.

Recently discovered with help of infrared device (Yuno project, 2018,[1]) cyclonic chains around both poles of Jupiter might be compared with famous catastrophic terrestrial cyclones. Jovian cyclones make chains of 8 around the North Pole and 5 around the South Pole. In case of Earth 8 tectonic granules of the wave nature and $\pi R/4$ size encircle the planet along the equator (grand planet's ring). At the western Pacific hemisphere four of these granules are presented by a chain of cyclones in the atmosphere (Fig.3). An essential difference of the jovian and terrestrial chains is in their positions: on Earth it belongs to the longest equatorial ring, on Jupiter to a much shorter ring in high latitudes near to the North Pole. Another important difference is in relative sizes of the storms (Fig. 4). On Earth they are smaller (as if, squeezed), on Jupiter they are larger, more massive. The positions of both chains should explain this taking into account difference of their angular momentum. The equatorial belt with the larger angular momentum requires squeezing objects to diminish momentum, the high latitude zones with smaller radius and momentum require more massive objects. All this for equilibration of momenta in various zones of a rotating body. Significantly squeezed terrestrial equatorial cyclones are catastrophically rapidly rotating.

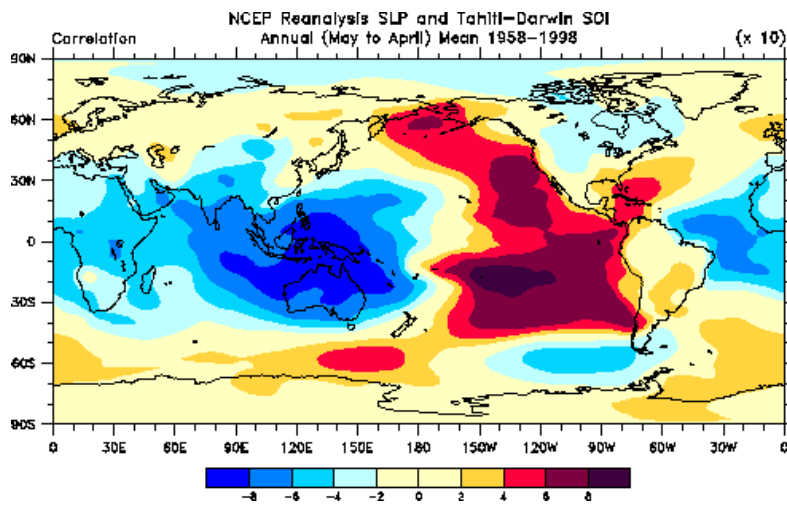
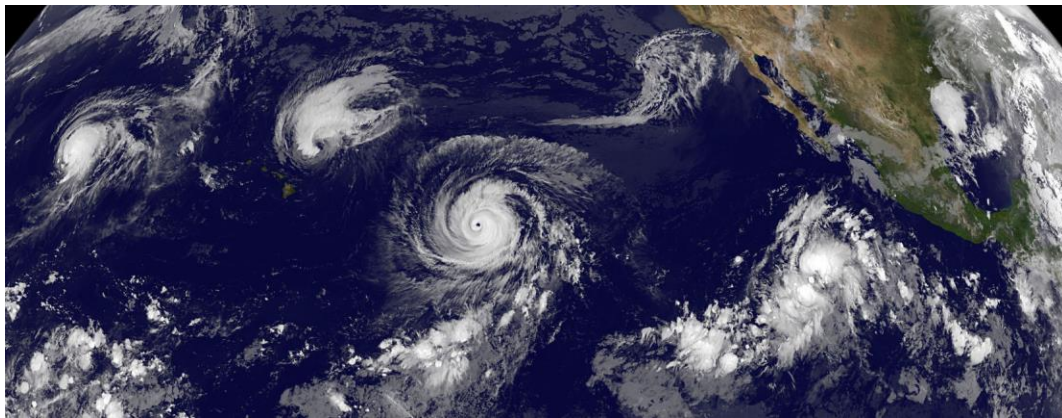


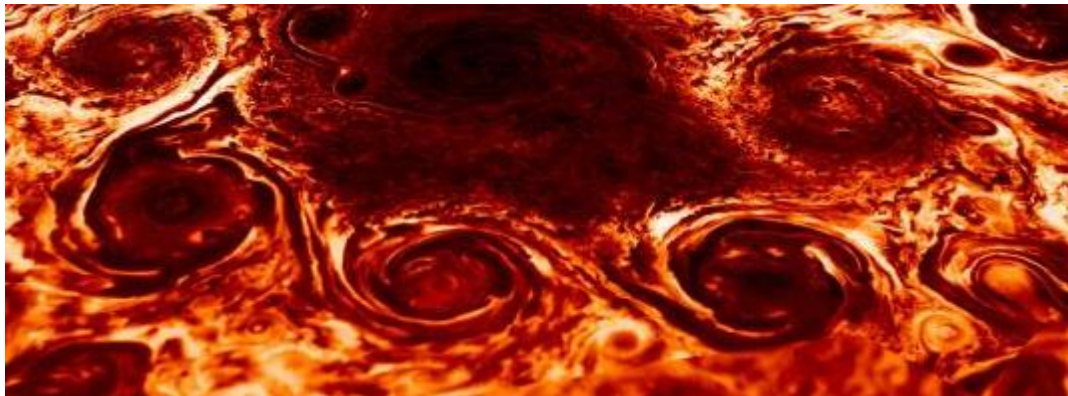
Fig. 1. High and low atmospheric pressures (many years observations) [1].



Fig. 2. Tornado in USA



3



4

Fig. 3. Cyclones on Earth. (over the Pacific). Fig. 4. Cyclones on Jupiter (North Pole) [2]

1. Adriani A., Muru A., Orton G., Hansen C., Altieri F et al Clusters of cyclones encircling Jupiter's poles // Nature, 2018, v. 555, # 7695, 216-219. doi:10.1038/nature25491

2. Trenberth K.E., P.D.Jones, P. Ambenje, R. Bojariu et al., 2007: Observations: Surface and Atmospheric Climate Change. In: Climate Change 2007: The Physical Science Basis. Contribution of Working Group I to the Fourth Assessment Report of the Intergovernmental Panel on Climate Change [Solomon S., D. Qin, M. Manning, Z. Chen, M. Marquis, K.B. Averyt, M. Tignor and M.L. Miller (eds.)] 2007, Cambridge University Press, Cambridge, United Kingdom and New York, NY. USA.

Electron and ion particle acceleration regimes observed by Juno over Jupiter's main aurora

Barry Mauk (1), Dennis Haggerty (1), Chris Paranicas (1), George Clark (1), Peter Kollmann (1), Abigail Rymer (1), Scott Bolton (2), Steven Levin (3), Alberto Adriani (4), F. Allegrini (2), Fran Bagenal (5), Bertrand Bonfond (6), John Connerney (7), Robert Ebert (2), Sadie Elliott (8), Randy Gladstone (2), William Kurth (8), Dave McComas (9), Drake Ranquist (5), Phil Valek (2)

- (1) The Johns Hopkins University Applied Physics Laboratory, Laurel, Maryland, USA (Barry.Mauk@jhuapl.edu)
- (2) Southwest Research Institute, San Antonio, Texas, USA
- (3) Jet Propulsion Laboratory, Pasadena, California, USA
- (4) Istituto Nazionale di Astrofisica-Istituto di Astrofisica e Planetologia Spaziali, Roma, Italy
- (5) Laboratory for Atmospheric and Space Physics, University of Colorado, Boulder, Colorado, USA
- (6) Laboratoire de Physique Atmosphérique et Planétaire, STAR Institute, Université de Liège, Belgium
- (7) NASA Goddard Space Flight Center, Greenbelt, Maryland, USA
- (8) Department of Physics and Astronomy, University of Iowa, Iowa City, Iowa, USA
- (9) Department of Astrophysical Sciences, Princeton University, Princeton, New Jersey, USA

Abstract

Over Jupiter's most intense main aurora, the Juno spacecraft has identified up to four different particle acceleration regimes at energies above 30 keV (not counting the diffuse auroras generally observed equatorward of the main aurora). 1) In many main auroral regions there are both upward and downward accelerated electron angle-beam-like distributions with broadband electron spectral characteristics, extending to > 1 MeV energies, without any signatures of magnetic field-aligned electric potentials. Because the most intense beam-like angular distributions generally reside within the magnetically determined loss cones, there is clear evidence of stochastic-like electron acceleration both upward at positions below the spacecraft (0.5-1.0 RJ) and downward at positions above the spacecraft. These distributions are sometimes accompanied by upward and/or downward proton angular beams and sometimes not. 2) Juno sometimes observes downward electron "inverted-V-like" distributions with peaked electron distributions indicative of upward electric potentials (up to 400 kV inferred). Generally the downward electron energy fluxes associated with such potentials are less than those associated with the stochastically accelerated electron distributions observed nearby. 3) Several times Juno has observed clear transitions between the downward electron inverted-V distributions and downward broadband electron distributions. The difference between these broadband electron distributions and

those identified as (1) above is that the apparent stochastic acceleration occurs primarily in the downward direction. 4) Finally, Juno sometimes observes strong downward ion inverted V's indicating the existence of downward electric potentials up to sometimes greater than 400 kV. The surprise here is that there also occurs simultaneously the upward and downward broadband acceleration of electrons such that the associated auroral emissions would be as intense as those observed in other regions. In this presentation we explore the characteristics of, and the relationships between, these different regimes with a particular focus on the relationship between electrons and ions. One of the surprises is that: A) downward ion inverted-V distributions are quite common within the main aurora with angular characteristic that suggest that they are accelerated downward at positions that are large distances upward away from the spacecraft, while B) downward ion inverted-V's have not been observed at radial positions greater than, say 4 RJ. This and other conundrums about the different auroral acceleration regimes are explored.

Observations of Jupiter by the Juno Ultraviolet Spectrograph (Juno-UVS)

Thomas K. Greathouse (1), G. Randall Gladstone (1), Vincent Hue (1), Maarten Versteeg (1), Bertrand Bonfond (2), Michael Davis (1), Denis C. Grodent (2), Jean-Claude Gérard (2), Joshua Kammer (1), Scott Bolton (1), Steven Levin (3), and John E.P. Connerney (4)
(1) Southwest Research Institute, Texas, USA, (2) STAR Institute, LPAP, Université de Liège, Liège, Belgium, (3) Jet Propulsion Laboratory, California, USA, (4) NASA Goddard Space Flight Center, Maryland, USA (tgreathouse@swri.edu)

Abstract

We present an overview of the science performed by Juno's Ultraviolet Spectrograph, UVS, over the first 11 successful perijove sequences performed since orbital insertion on July 4th, 2016. In particular, we will discuss 1) the measured local time dependence of Jupiter's polar auroral emissions, 2) simultaneous UV and H₃⁺ observations and their correlations or lack thereof, 3) the evolution and morphology of Io's magnetic footprint in Jupiter's atmosphere, 4) measurements concerning the spatial and temporal variation of high energy particles (>10 MeV) in the polar regions of Jupiter's magnetosphere, and 5) the production of an all sky UV stellar atlas at wavelengths between 68 and 210 nm.

1. Introduction

Juno [1] is a NASA New Frontiers mission currently on a highly elliptical polar orbit around Jupiter, since 4 July 2016, and has successfully gathered science data during 11 perijove sequences. It offers a unique opportunity to measure in situ particles and fields simultaneously with remote sensing of H₃⁺ and UV auroral emissions. These emissions serve as a viewing screen for the events and dynamics occurring throughout much of the Jovian magnetosphere. The Juno Ultraviolet Spectrograph (UVS) [2] is a UV spectrograph, with a bandpass spanning 68 to 210 nm, designed to characterize Jupiter's UV emissions. In this presentation we offer an overview of results obtained from using UVS through the first 11 perijoves of the mission.

2. Results

2.1 Local time variations of auroral polar emissions

Juno-UVS measurements of the night side aurora have revealed a pronounced local time effect on polar auroral emissions, i.e., within the main auroral oval. Previous ground-based observing campaigns have shown that this polar auroral region is very structured, with distinct regions characterized by high color ratios (i.e. deeper UV emissions). Juno allows us to characterize, for the first time, the day/night variations of these polar auroral emissions, providing insights on the ionospheric / outer-magnetospheric coupling.

2.2 Comparisons of UV emissions and Near-infrared H₃⁺ emissions

Simultaneous views of the entire Jovian aurorae at high spatial resolutions in the UV and NIR shed light on correlations between these two types of emission [3]. Although both auroras ultimately result from the precipitation of energetic electrons, the prompt nature of the H₂ and H UV transitions versus the more circuitous H₃⁺ emission mechanism leads to some very distinct differences between them.

2.3 Variability of Io's footprint

Previous observations by the Hubble Space Telescope allowed the characterization of the Io footprints as a function of Io's centrifugal latitude, despite the observational bias of Earth-based viewing. Juno's unique vantage point in the Jovian system removes these biases allowing UVS access to the full range of Io's centrifugal latitude for all possible local time geometries. We will present results on the

variability of the footprint emitted power as a function of Io's system III longitude and local time.

2.4 High Energy radiation in Jupiter's polar environment

Juno-UVS is sensitive to high-energy electrons and gamma-rays (>10 MeV) providing another way for Juno to probe Jupiter's radiation environment. These measurements are used to (i) refine radiation models of Jupiter, (ii) improve future Juno-UVS observation planning by providing an empirical model of the radiation levels and (iii) to provide high-cadence measurements of the radiation in the polar auroral region, in support of Juno's particle instruments.

2.5 All sky map in the Ultraviolet

As a side effect of Juno's spin, Juno-UVS also provides a rich dataset of the stellar and galactic UV emission in the 68 to 210 nm bandpass. More than 99% of the sky has been mapped since launch, with an accumulated integration time greater than 1 hour in several regions of the sky.

3. Summary and Conclusions

During its first 11 of the planned 32 orbits, Juno has produced a treasure trove of new results, baffling scientific conundrums, and exquisite imagery sparking the imagination. We look forward to how the future orbits of Juno will further inform our understanding of Jupiter's atmosphere and magnetosphere.

Acknowledgements

We gratefully acknowledge NASA funding for the Juno Mission and the UVS instrument team specifically.

References

- [1] Bolton, S.J., et al., The Juno Mission. *Space Science Reviews*, 213, pp. 5-37, 2017.
- [2] Gladstone, G.R., et al., The Ultraviolet Spectrograph on NASA's Juno Mission. *Space Science Reviews*, 213, p. 447-473, 2017.
- [3] Gérard, J.-C., et al., Concurrent ultraviolet and infrared observations of the north Jovian aurora during Juno's first perijove. *Icarus*, 312, pp. 145–156, 2018.

Juno Maps Jupiter's Planetary Magnetic Field

J. E. P. Connerney (1,2), R. J. Oliverson (2), J. R. Espley (2), D. J. Gershman (2,3), S. Kotsiaros (2,4), Y. Martos (2,3), J. L. Joergensen (5), P. S. Joergensen (5), J. M. G. Merayo (5), T. Denver (5), M. Benn (5), J. Bloxham (6), K. M. Moore (6), S. J. Bolton (7), S. M. Levin (8)

(1) Space Research Corporation, Annapolis, MD, USA, (2) NASA Goddard Space Flight Center, Greenbelt, MD, USA, (3) University of Maryland, College Park, MD, USA, (4) Universities Space Research Association, Columbia, MD, USA, (5) Technical University of Denmark (DTU), Lyngby, Denmark, (6) Harvard University, Cambridge, MA, USA, (7) Southwest Research Institute, San Antonio, TX, USA, (8) Jet Propulsion Laboratory, Pasadena, CA, USA, (jack.connerney@nasa.gov)

Abstract

The Juno spacecraft entered polar orbit about Jupiter on July 5 (UTC), 2016, in search of clues to the planet's formation and evolution. Juno probes the deep interior with measurements of Jupiter's magnetic and gravitational potential fields, acquired during close periapsis passes that occur every ~53 days. Thus far, Juno has acquired 15 of the planned 34 orbits needed to complete its global map.

Juno's baseline mission plan [1,3] was designed, in part, to wrap the planet in a dense net of observations in close proximity, approximating measurements on a closed surface about the source (Fig 1), ideal for characterizing potential fields [5].

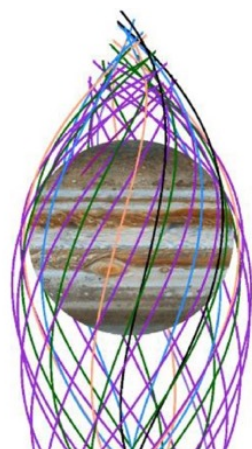


Figure 1: Juno wraps the planet in a dense net of observations, with 34 passes to within ~1.06 R_J .

Repeated periapsis passes will eventually wrap the planet with observations equally spaced in longitude ($<12^\circ$ at the equator), optimized for characterization of the Jovian dynamo. Such close passages are sensitive to small spatial scale variations in the magnetic field and a large number of such passes is required to bring the magnetic field into focus. The first 9 periapsis passes revealed a magnetic field rich in higher harmonic content [7], suggestive of magnetic dynamo action not far beneath the surface [4,7,8]. It is perhaps not surprising that the field observed in close proximity to the planet is very different from that predicted by existing models, necessarily limited to low harmonic degree and order.

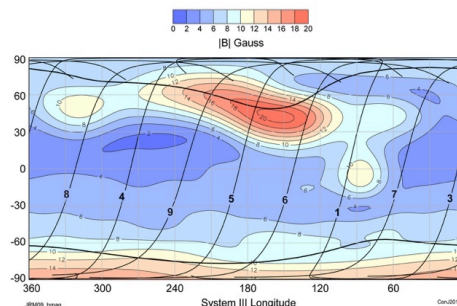


Figure 2: Magnetic field magnitude on the flattened surface of Jupiter computed using the JRM09 model magnetic field, based on Juno's first nine (numbered) orbits. Unlabeled curve shows the path of the Io flux tube footprint in both hemispheres.

The magnetic field investigation (MAG) [5] is equipped with two magnetometer sensor suites, located 10 & 12 m from the center of the spacecraft at the end of one of Juno's three solar panel wings. Each contains a vector fluxgate magnetometer (FGM)

sensor and a pair of co-located non-magnetic star tracker camera heads, providing accurate attitude determination for the FGM sensors. These cameras monitor the distortion of the mechanical appendage (solar array and MAG boom) in real time, allowing accurate attitude reconstruction for the FGM sensors to ~ 20 arcsec throughout the mission [5]. They have also proven valuable in characterizing dust impacts on the Juno spacecraft as it transited the solar system en route to Jupiter [2].

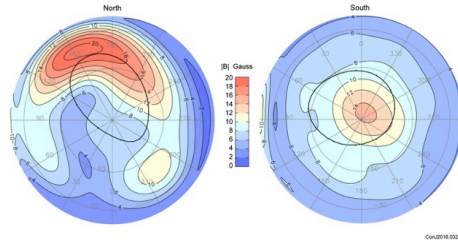


Figure 3: Orthographic projection of the magnetic field magnitude computed using the JRM09 magnetic field model on Jupiter's flattened surface. Ovals show the path of the Io flux tube footprint computed using the same model.

Jupiter's planetary magnetic field is modeled using a spherical harmonic representation of the internal magnetic field, combined with an explicit model of the field due to external currents (Jovian magnetodisc) [7]. Thus far in the mission, global coverage remains rather sparse, so we solve the inverse problem using generalized inverse methods that allow a partial solution to a high-degree spherical harmonic expansion for the internal field. Thus far, spherical harmonic coefficients through degree and order 10 can be resolved, using a basis model through degree 20, required to follow spatial variations on the field observed during close passage.

Jupiter's magnetic field at current resolution is remarkable in its hemispherical asymmetry, with the northern hemisphere characterized by abundant non-dipolar fields and the southern hemisphere very dipolar in appearance (see figure 3). The field geometry also dictates interesting charged particle motions in close proximity to the planet, with drift shells lacking closure external to the planet at equatorial field strengths of ~ 2 Gauss. We present an overview of the magnetic field observations obtained during the first two years of Juno's mapping mission

in context with prior observations and those acquired by Juno's other science instruments.

References

- [1] Bagenal, F., Adriani, A., Allegrini, F., et al.: Magnetospheric science objectives of the Juno mission, *Space Sci. Rev.*, doi 10.1007/s11214-014-0036-8.
- [2] Benn, M., Jorgensen, J. L., Denver, T., et al. (2017): Observations of interplanetary dust by the Juno magnetometer investigation, *Geophys. Res. Lett.*, ., 44, doi: [10.1002/2017GL073186](https://doi.org/10.1002/2017GL073186).
- [3] Bolton, S. J. and the Juno Science Team (2010). The Juno mission. *Proceedings of the International Astronomical Union Symposium*, No. 269: 92-100.
- [4] Bolton, S. J., Adriani, A., Adumitroaie, V., et al.: Jupiter's interior and deep atmosphere: the first pole-to-pole pass with the Juno spacecraft, *Science*, doi: 10.1126/science.aal2108, 2017.
- [5] Connerney, J. E. P., Benn, M., Bjarno, et al. (2017) The Juno Magnetic Field Investigation, *Space Sci. Rev.*, doi: 10.1007/s11214-017-0334-z.
- [6] Connerney, J. E. P., Adriani, A., Allegrini, F., et al. (2017): Jupiter's Magnetosphere and Aurorae Observed by the Juno Spacecraft During its First Polar Orbits, *Science*, 10.1126/science.aam5928.
- [7] Connerney, J.E.P., Kotsiaros, S., Oliverson, R.J., Espley, J.R., Joergensen, J.L., Joergensen, P.S. et al., (2018). A new model of Jupiter's magnetic field from Juno's first nine orbits. *Geophysical Research Letters*, 45, doi: 10.1002/2018GL077312.
- [8] Moore, K. M., Bloxham, J., Connerney, J. E. P., et al. (2017): The analysis of initial Juno magnetometer data using a sparse magnetic field representation, *Geophys. Res. Lett.*, 44, doi: [10.1002/2017GL073133](https://doi.org/10.1002/2017GL073133).

Latest Results on Jupiter's Atmosphere and Radiation Belts from the Juno Microwave Radiometer

Glenn S. Orton (1), Michael A. Janssen (1), Scott J. Bolton (2), Steven M. Levin (1), Virgil Adumitroaie (1), Michael D. Allison (3), John K. Arballo (1), Sushil K. Atreya (4), Amadeo Bellotti (5), Shannon T. Brown (1), Samuel Gulkis (1), Andrew P. Ingersoll (6), Cheng Li (6), Liming Li (7), Jonathan Lunine (8), Sidharth Misra (1), Fabiano A. Oyafuso (1), Daniel Santos-Costa (2), Edwin Sarkissian (1), Paul G. Steffes (5), Fachreddin Tabataba-Vakili (1), and Zhimeng Zhang (6)
(1) Jet Propulsion Laboratory, California Institute of Technology, Pasadena CA 91108
(2) Southwest Research Institute, San Antonio TX 78228
(3) Goddard Institute of Space Studies, New York NY 10025
(4) University of Michigan, Ann Arbor MI 48109
(5) Georgia Institute of Technology, Atlanta GA 30332
(6) California Institute of Technology, Pasadena CA 91125
(7) University of Houston, Houston TX 77004
(8) Cornell University, Ithaca NY 14853

Abstract

The Juno Microwave Radiometer (MWR) was designed to investigate Jupiter's atmosphere and radiation belts as one of a suite of instruments that form the core of the Juno mission [1]. Results from the first fourteen periapsis passes on the atmosphere and the radiation belts will be summarized.

1. Introduction

Jupiter's neutral atmosphere is shrouded by clouds that are impervious to all but microwave radiation. Our view from Earth is impeded further by intense synchrotron radiation that obscures all but the shortest-wavelength microwave radiation emanating from above the few-bar pressure level of the atmosphere. Juno's highly elliptical polar orbit allows the MWR to avoid these obstacles by observing the atmosphere during a periapsis pass from a vantage point between Jupiter and the radiation belts. This enables the measurement of longer-wavelength atmospheric thermal radiation from pressure depths of hundreds of bars, and also provides a unique view of the inner radiation belts that enables a more complete study of their structure.

2. Observational Approach

The MWR comprises six radiometric channels operating at wavelengths from 1.4 cm to 50-cm wavelength. The MWR antennas are mounted on the sides of the spinning Juno spacecraft so that they observe along the subspacescraft track as the spacecraft

moves from north to south through periapsis. Collectively they sample the thermal emission from pole to pole with better than 1° resolution in latitude at periapsis, and from the cloud tops to pressures as deep as a few hundred bars.

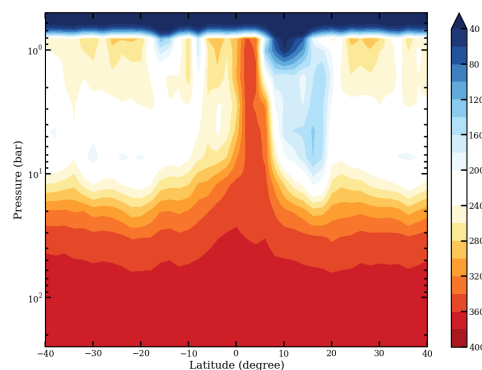


Figure 1: Ammonia abundance (ppm) derived from MWR observations on periapsis 1 [3].

The observational data are the mean radiances in the antenna beams converted by Planck's law to blackbody temperatures and accordingly given in units of Kelvin (antenna temperatures). For atmospheric data, these are corrected for the beam averaging to obtain source brightness temperatures, or the effective mean radiance of Jupiter in the beam at the boresight axis, for each observation. The absolute accuracy of each measurement is 2%, uncorrelated among channels, while the relative accuracy at each

wavelength is 0.1%. The radiation belt data consist of antenna temperatures from latitudinal scans from a (mostly) radiation-free perspective inside the belts.

3. Data Products

The atmospheric scans along the sub-spacecraft track yield both absolute brightness temperatures and, since many points are observed over a range of emission angles, their dependence on emission angle. The data products derived from these data include latitudinal tracks of absolute nadir brightness temperatures, where off-nadir measurements are extrapolated to nadir using their simultaneously-obtained emission angle dependencies; and emission angle dependence in terms of limb-darkening parameters. The former are useful in the determination of large-scale structure in the subcloud atmosphere due to opacity variations, which are not limited by 2% absolute uncertainties. These also are useful in the constructions of partial 3D maps, which show brightness structure as a function of latitude, longitude, and wavelength (a proxy for depth). Emission-angle dependencies allow fine structure with depth to be obtained with accuracy limited only by the 0.1% relative accuracies of the measurements at each wavelength. The radiation belt data consist of antenna temperatures from latitudinal scans from a radiation-free perspective inside the belts, useful for comparison with synthetic data obtained by computations using parameterized models of the belts.

4. Results

The trace of absolute nadir brightness temperature for the first perijove pass has been used to infer a striking variation in the distribution of NH_3 , which is the dominant source of microwave opacity in the atmosphere [2]. This variation implies a previously unexpected deep circulation (Fig. 1) with exciting implications for gas-giant planets in general [3].

The accumulation of data from subsequent perijove passes will be shown to demonstrate the longitudinal, temporal, and depth dependencies of observed structures. Multiple perijove passes show temporal and longitudinal repeatability of all the major features, as well as identifying a few specific features which are unique to a particular longitude. Partial 3D maps will show the structure and depths of specific features on Jupiter, notably the polar regions and the Great Red Spot. Finally, efforts underway to determine the water abundance will be described.

Acknowledgements

The work described in this paper was conducted at the Jet Propulsion Laboratory (JPL), California Institute of Technology, under contract with the National Aeronautics and Space Administration (NASA). The author wishes to thank the numerous contributors from the Juno Project and the Lockheed-Martin spacecraft team, without whom this ambitious project would not have been possible.

References

- [1] Janssen, M. A., et al., MWR: Microwave Radiometer for the Juno Mission to Jupiter. 2017. *Space Science Reviews*, **213**, 139-185, 2017, doi: 10.1007/s11214-017-0349-5.
- [2] Bolton, S.J. et al., Jupiter's interior and deep atmosphere: the first close polar pass with the Juno spacecraft. 2017. *Science*, **356**, 821-825. doi: 10.1126 / science.aal2108.
- [3] Li, C. et al. The distribution of ammonia on Jupiter from a preliminary inversion of Juno Microwave Radiometer data. 2017. *Geophysical Research Letters*, **44**, 5317-5325 doi: 10.1002 / 2017GL073159.

How deep is the Great Red Spot? Determining the depth of the GRS with the Juno gravity measurements

Eli Galanti (1), Yohai Kaspi (1), Marzia Parisi (2), and William M. Folkner (2)

(1) Weizmann Institute of Science, Rehovot, Israel, (2) Jet Propulsion Laboratory, California Institute of Technology, Pasadena, California

Abstract

Jupiter's Great Red Spot (GRS) is the most dominant and long-lived feature in Jupiter's atmosphere. However, whether this is a shallow atmospheric feature or a deeply rooted vortex has remained an open question. The recent gravity measurements, performed by the Juno mission, enabled the analysis of Jupiter's zonal flows that were found to penetrate to depth of 3,000km below the cloud-level. This analysis was based on several Juno tracks in which high precision gravity measurements were obtained, alas none of them went over the GRS. The only Juno perijove to date to occur over Jupiter's GRS (PJ7) was devoted to determining ammonia and water abundance in the region, resulting in a gravity measurement based on a lower quality signal. The microwave analysis indicated that the winds in the GRS region extend to depth of at least a couple hundred kilometers, placing a lower limit on the depth of the winds there but not an upper one.

Here we present results of the gravity analysis of the PJ7 gravity measurements and use it to constrain the mass density variations associated with the GRS. Moreover, we discuss the potential of additional gravity overflights to provide stronger constraints on the structure of the GRS and its vertical extension below the cloud tops. We explore the possible gravitational signature of the vortex by systematically extending the surface winds into the interior and analyzing the resulting density perturbations. The flow-density relation is based on a thermal wind balance in both the zonal and meridional components of the wind, enabling the calculation of the full horizontal density gradients resulting from a given flow structure. The density gradients are used to calculate different scenarios of gravity anomalies that are then compared to the expected accuracy in potential gravity measurements at the GRS location.

Juno Waves observations at Jupiter

W. S. Kurth (1), G. B. Hospodarsky (1), M. Imai (1), S. S. Elliott (1), D. A. Gurnett (1), P. Louarn (2), P. Valek (3,4), F. Allegrini (3,4), J. E. P. Connerney (5), B. H. Mauk (6), S. J. Bolton (3), S. M. Levin (7), A. Adriani (8), G. R. Gladstone (3,4), D. J. McComas (3,9), P. Zarka (10), C. Louis (10)

(1) University of Iowa, Iowa City, IA, USA, (2) IRAP, Toulouse, France, (3) Southwest Research Institute, San Antonio, TX, USA, (4) Department of Physics and Astronomy, University of Texas at San Antonio, San Antonio, TX, USA, (5) NASA Goddard Space Flight Center, Greenbelt, MD, USA, (6) The Johns Hopkins University Applied Physics Laboratory, Laurel, MD, USA, (7) Jet Propulsion Laboratory, Pasadena, CA, USA, (8) INAF-Istituto di Astrofisica e Planetologia Spaziali, Roma, Italy, (9) Princeton University, Princeton, NJ, USA, (10) LESIA, Observatoire de Paris, Meudon, France.

Abstract

The Juno spacecraft successfully entered Jupiter orbit on 5 July 2016. One of Juno's primary objectives is to explore Jupiter's polar magnetosphere. An obvious major aspect of this exploration includes remote and in situ observations of Jupiter's auroras and the processes responsible for them. To this end, Juno carries a suite of particle, field, and remote sensing instruments. One of these instruments is a radio and plasma wave instrument called Waves, designed to detect one electric field component of waves in the frequency range of 50 Hz to 41 MHz and one magnetic field component of waves in the range of 50 Hz to 20 kHz. Juno has now made scientific observations on several perijove passes beginning with Perijove 1 on 27 August 2016. This paper will focus on waves observed on or near auroral field lines.

Auroral radio emissions known as kilometric, hectometric, and decametric emissions have been

observed even at or close to their sources. Analysis of Jovian Auroral Distributions Experiment (JADE) electron distributions show sources of free energy sufficient to drive the cyclotron maser instability that is responsible for Jupiter's auroral radio emissions. Remote observations provide source locations for broadband kilometric radiation that are consistent with auroral field lines and UV auroras. Auroral crossings are often marked by auroral hiss emissions with a characteristic funnel shape presumably due to propagation near the resonance cone. This whistler-mode hiss is particularly intense when the Jupiter Energetic particle Detector (JEDI) observes very intense precipitating electrons with a broad energy spectrum extending up to 1 MeV. Lower frequency waves, below the proton cyclotron frequency, are also often observed with intensities greater than those at higher frequencies, suggesting ion-cyclotron waves. We will summarize the major wave phenomena on auroral field lines and attempt to assess their roles in the physics of Jupiter's auroras.

First measurements of the Jovian zonal winds profile through visible Doppler spectroscopy

François-Xavier Schmider (1), Ivan Gonçalves (1), Patrick Gaulme (2,3,4), Raúl Morales-Juberías (4), Tristan Guillot (1), Jean-Pierre Rivet (1), Thierry Appourchaux (5), Patrick Boumier (5), Jason Jackiewicz (3), Thomas A Underwood (3), David Voelz (3), Bun'ei Sato (6), Shigeru Ida (6), Masahiro Ikoma (7)

(1) Laboratoire Lagrange, Université Côte d'Azur, UMR 7293, Observatoire de la Côte d'Azur (OCA), Nice, France, (2) Max-Planck-Institut für Sonnensystemforschung, Justus-von-Liebig-Weg 3, 37077, Göttingen, Germany, (3) Department of Astronomy, New Mexico State University, P.O. Box 30001, MSC 4500, Las Cruces, NM 88003-8001, USA, (4) Physics Department, New Mexico Institute of Mining and Technology, 801 Leroy Place, Socorro, NM 87801, USA, (5) Institut d'Astrophysique Spatiale, Université Paris Sud, 91405 Orsay Cedex, France, (6) Tokyo Institut of Technology, Dept. of Earth and Planetary Sciences, 2-12-1 Ookayama, Meguro, Tokyo 152-8551, Japan, (7) Tokyo 113 Department of Earth and Planetary Science, The University of Tokyo, 7-3-1 Hongo Bunkyo-ku, -0033, Japan
(schmider@oca.eu)

Abstract

We present the first measurements of Jupiter's wind profile obtained from radial-velocity measurements. Radial velocity measurements of wind are rather difficult, but can be very interesting as they measure the actual speed of cloud particles instead of the motion of large cloud structures. Here we present the first scientific results of the Doppler spectro-imager JOVIAL-JIVE, dedicated to giant planets' seismology and atmospheric dynamics. The instrument provides instantaneous velocity maps in the mid-visible domain by monitoring the Doppler shift of solar Fraunhofer lines reflected in the planets' upper atmosphere thanks to an imaging Fourier transform spectrometer. We present profiles of the zonal wind speed of Jupiter as function of latitude from observations obtained between 2015 and 2017. Our results are compared with wind profiles obtained by cloud tracking from HST images at the same epoch. We point out comparable results from both techniques except at the latitude of the hot spots in the northern equatorial band ($\approx 5^\circ$ N) where we find a much lower wind speed.

1. Introduction

The *Juno* NASA spacecraft, which has been orbiting Jupiter since July 2016, aims at investigating the internal structure below the surface of the planet by measuring the gravitational moments. Very accurate values have been obtained so far [1]. However, interpret-

ing these measurements depends on our ability to correctly model the dynamics of the surface layers, as the moments are sensitive to both local composition gradients and to underlying differential rotation, which are not easy to disentangle. Thus, accurate measurements of the dynamics of Jupiter's upper atmosphere are fundamental for interpreting *Juno*'s data.

In this paper, we present the first measurements of Jupiter's atmospheric zonal winds obtained with Doppler imaging spectroscopy in the visible domain. As we discuss in the next section, measuring atmospheric winds with radial-velocity techniques brings unique information, complementary to the traditional cloud tracking results.

2. Observations and results

2.1. Instrumental concept

The Doppler Spectro-Imager (DSI) is an instrument that produces radial velocity maps of extended objects. The instrument is a compact Mach-Zehnder (MZ) interferometer with a fixed Optical Path Difference (OPD) which provides four interferograms, whose fringes phase measures the Doppler shift of Fraunhofer lines between 519 and 520 nm. Its concept and performances are described in [2]. The instrument was developed in the context of the JUICE mission and a prototype was realized in this goal, which was tested on the sky in 2013. A new joint project (JOVIAL-JIVE) started in 2014 to set-up a network of three instruments around the Earth for continuous ob-

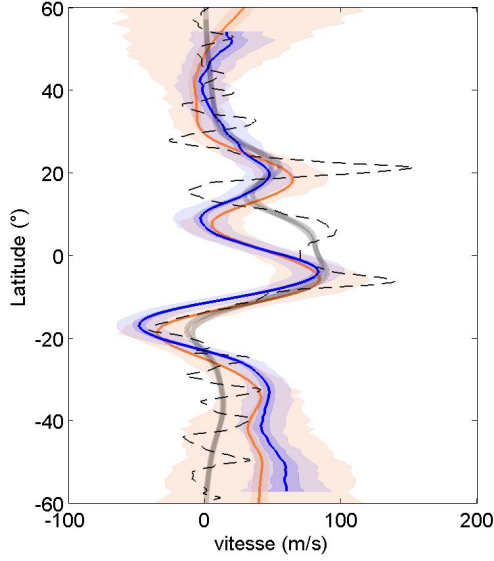


Figure 1: Zonal winds profile of Jupiter obtained with the Doppler Spectro Imager in 2016 (orange) and 2017 (blue) as compared with cloud-tracking measurements from HST data in 2016 (dashed line). For a better comparison, we simulated a degraded wind profile from cloud-tracking using the same PSF as the DSI observations and shown here as gray lines.

servations. Here, we report observations carried out with the JOVIAL-JIVE instrument at the C2PU 1m telescope at Calern observatory near Nice. Observations were obtained near Jovian’s opposition in Mars 2016 and April 2017.

2.2. Results

We show here the result from about 10 nights in 2016 and only one night in 2017. Images were obtained at a rate of two per minutes. The phase of the interferometric fringes is corrected from the instrumental phase, obtained on the diffused solar light during the day to produce a velocity map. A solid rotation model is first applied, then a linear fit along each line parallel to the equator on the remaining velocity map gives the mean zonal velocity as a function of the latitude. The spatial resolution is limited by the atmospheric seeing around 2 to 3 arcsec. The dispersion of these measurements is displayed in light color for each year, and compared to the theoretical photon noise in darker color.

Our zonal winds estimates are in complete agree-

ment each year. We compare them with simulated Doppler measurements using the same angular resolution as DSI observations assuming that the actual velocity corresponds to cloud-tracking wind profile from HST observations [3]. Zonal profile from Doppler imaging are compatible with cloud-tracking zonal velocity profile, except in the northern equatorial band, between 0 and 15 degrees north, where a significative discrepancy can be seen. Several hypothesis can be formulated to explain this difference. Either the Doppler measurements can be sensitive to other components of the wind [4], or we are looking at different altitude, or the cloud-tracking itself doesn’t reflect the actual particle speed. It has to be noticed that the northern equatorial band is known to exhibits almost periodic hotspots. These hotspots have been interpreted as the effect of Rossby waves, travelling westward upon faster jets [5]. Our measurements are apparently in contradiction with this interpretation but more has to be done to confirm our observations. We foresee new observations with a better angular resolution. However, it would be interesting to look for an interpretation of the Juno’s data assuming a surface wind velocity compatible with our results.

Acknowledgements

This work has been supported by the ANR JOVIAL and the JIVE in NM EPSCOR NASA programme. We thank the C2PU telescope team in Calern Observatory for valuable help.

References

- [1] Bolton, S. J. et al, Jupiter’s interior and deep atmosphere: The initial pole-to-pole passes with the Juno spacecraft. *Science* 356, 821–825 (2017)
- [2] Gonçalves, I. et al, Advances in the development of a Mach-Zehnder interferometric Doppler imager for seismology of giant planets, in *SPIE 9908*, 99083M (2016)
- [3] Johnson, P. E. et al, Longitudinal variability in jupiter’s zonal winds derived from multi-wavelength HST observations, *Planetary and Space Science*, in press (2018)
- [4] Gaulme, P., Schmider, F.-X., and Goncalves, I.: Measuring planetary atmospheric dynamics with Doppler spectroscopy, *A&A*, in press (2018)
- [5] Choi, D. S. et al, Meteorology of Jupiter’s equatorial hot spots and plumes from Cassini, *Icarus*, 223, 832 (2013)

The New Jupiter as Revealed by Juno

S. Bolton (1), J. Connerney (2,3), S. Levin (3) and the Juno Science Team

(1) SWRI, San Antonio, United States, (2) Space Research Corporation, Annapolis, USA, (3) JPL, Caltech, Pasadena, United States

Abstract

Juno is the first mission to investigate Jupiter using a close polar orbit. The Juno science goals include the study of Jupiter interior composition and structure, deep atmosphere and its polar magnetosphere. All orbits have perijove at approximately 5000 km above Jupiter's visible cloud tops. The payload consists of a set of microwave antennas for deep sounding, magnetometers, gravity radio science, low and high-energy charged particle detectors, plasma wave antennas, ultraviolet imaging spectrograph, infrared imager and spectrometer and a visible camera.

1. Introduction

The primary science goal of Juno is the understanding of the origin and evolution of Jupiter, the history of our solar system and the more general theory of planetary system formation. To address these goals, Juno probes significantly below the cloud decks to constrain its interior structure using measurements of Jupiter's gravity and magnetic fields and deep atmospheric composition [1]. Juno's elliptical orbit provides multiple periapsis passes very close to Jupiter, on a pole-to-pole trajectory. The very close-in polar orbits enable a unique exploration of Jupiter's polar magnetosphere [2]. Juno's payload of science investigations include an X-band and Ka-band communications subsystem for determining Jupiter's gravity field, dual magnetometers to map Jupiter's internal magnetic field, a set of microwave radiometers to probe Jupiter's deep atmosphere, a visible color camera and an infrared spectrometer/imager and ultraviolet spectrograph/imager to capture views of Jupiter. Juno also carries a suite of fields and particle instruments for in-situ sampling Jupiter's magnetosphere and investigating its powerful aurora [2].

2. Science Results

On July 4, 2016, the Juno spacecraft arrived at Jupiter to begin the investigation of Jupiter. The spacecraft acquired science observations of Jupiter, passing within 3000 km of the equatorial cloud tops. Images of Jupiter's poles indicate cyclonic activity unique to the solar system. Microwave sounding reveals weather features, dominated by an ammonia-rich, narrow low-latitude plume. Near-infrared mapping reveals the relative humidity within prominent down-welling regions. Juno's measured gravity field differs significantly from the current knowledge and is one order of magnitude more precise. This has implications for the distribution of heavy elements in the interior including the existence and mass of Jupiter's core. The observed magnetic field exhibits smaller spatial variations than expected. Direct observations of the Jovian polar magnetosphere provide the first close-up observations of Jupiter's auroral regions. Energetic particle and plasma detectors measured electrons precipitating in the polar regions, exciting intense aurorae, observed simultaneously by the ultraviolet and infrared imaging spectrographs.

Acknowledgements

The authors acknowledge financial support from the Juno project under NASA, CNES and ASI.

References

- [1] Bolton, S. J., Adriani, A., Adumitroaie, V., et al.: Jupiter's interior and deep atmosphere: the first pole-to-pole pass with the Juno spacecraft, *Science*, in press, 2017.
- [2] Connerney, J., Adriani, A., Allegrini, F., et al.: Jupiter's Magnetosphere and Aurorae Observed by the Juno Spacecraft During its First Polar Orbits, *Science*, in press, 2017.

Energetic proton and heavy ion observations over Jupiter's main auroral and polar cap regions

G. Clark (1), B.H. Mauk (1), D. Haggerty (1), P. Kollmann (1), C. Paranicas (1), A. Rymer (1), D.G. Mitchell (1), F. Allegrini (2,3), R.W. Ebert (2), G. Hospodarsky (4), W.S. Kurth (4), J. Saur (5) P. Valek (2,3), S. Bolton (2), J.E.P. Connerney (6,7), S. Levin (8)

- (1) The Johns Hopkins University Applied Physics Laboratory, Laurel, Maryland, USA
- (2) Southwest Research Institute, San Antonio, Texas, USA
- (3) Physics and Astronomy Department, University of Texas at San Antonio, Texas, USA
- (4) University of Iowa, Iowa City, Iowa, USA
- (5) Institut für Geophysik und Meteorologie, Universität zu Köln, Köln, Germany
- (6) Space Research Corporation, Annapolis, MD
- (7) NASA Goddard Space Flight Center, Greenbelt, Maryland, USA
- (8) Jet Propulsion Laboratory, Pasadena, California, USA

Abstract

Proton and heavy ion observations from Juno's energetic particle instrument, JEDI, reveal a host of processes occurring near the main auroral oval and in regions poleward of the oval. Some of the first studies from [1,2,3,4] showed evidence for precipitating energetic heavy ions into Jupiter's atmosphere as well as magnetic field-aligned electric potentials accelerating protons and heavier ions to several MeV and energetic proton conics formed by the "pressure cooker" effect. More recent observations from the previous twelve auroral passes (PJ1-PJ12) continue to show clear examples of MV electric potentials and energetic proton conics – giving us the ability to further characterize these processes. Additionally, recent analysis also reveals the presence of upward beaming heavier ions with energies extending well into the 100s of keV and MeV with angular profiles consistent with that of the proton conics. How these energetic heavier ions, such as helium, oxygen and sulfur, are entrained in this physical process is explored. In this presentation, we will also discuss some recent examples of large-scale MV

electric-potential structures over the polar cap region.

References

- [1] Mauk, B. H., Haggerty, D. K., Paranicas, C., Clark, G., Kollmann, P., Rymer, A. M., ... Valek, P. (2017a). Juno observations of energetic charged particles over Jupiter's polar regions: Analysis of monodirectional and bidirectional electron beams. *Geophysical Research Letters*, 44(10), 4410–4418. <https://doi.org/10.1002/2016GL072286>
- [2] Haggerty, D. K., Mauk, B. H., Paranicas, C. P., Clark, G., Kollmann, P., Rymer, A. M., ... Levin, S. M. (2017). Juno/JEDI observations of 0.01 to >10 MeV energetic ions in the Jovian auroral regions: Anticipating a source for polar X-ray emission. *Geophysical Research Letters*, 44(13), 6476–6482. <https://doi.org/10.1002/2017GL072866>
- [3] Clark, G., Mauk, B. H., Paranicas, C., Haggerty, D., Kollmann, P., Rymer, A., ... Valek, P. (2017b). Observation and interpretation of energetic ion conics in Jupiter's polar magnetosphere. *Geophysical Research Letters*, 44(10), 4419–4425. <https://doi.org/10.1002/2016GL072325>
- [4] Clark, G., Mauk, B. H., Haggerty, D., Paranicas, C., Kollmann, P., Rymer, A., ... Valek, P. (2017a). Energetic particle signatures of magnetic field-aligned potentials over Jupiter's polar regions. *Geophysical Research Letters*, 44(17), 8703–8711. <https://doi.org/10.1002/2017GL074366>

Short-term and long-term variability of Jupiter's auroral stratosphere

James A. Sinclair (1), Glenn S. Orton (1), Thomas K. Greathouse (2), Yasumasa Kasaba (3), Takao Sato (4), Rohini S. Giles (1), Henrik Melin (5), Leigh N. Fletcher (5), Julianne I. Moses (6), Patrick. G. J. Irwin (7)
(1) Jet Propulsion Laboratory/Caltech, United States (james.sinclair@jpl.nasa.gov), (2) Southwest Research Institute, United States
(3) Tohoku University, Japan, (4) Japanese Aerospace Exploration Agency (JAXA), Japan, (5) University of Leicester, United Kingdom, (6) Space Science Institute, United States, (7) University of Oxford, United Kingdom.

Abstract

We will present an analysis of multiple datasets, which capture the mid-infrared stratospheric emission of Jupiter's auroral regions on different timescales. A time series of 7.8- μm CH_4 emission images measured by Subaru-COMICS as well as high-resolution spectral measurements of CH_4 , C_2H_2 , C_2H_4 and C_2H_6 emission recorded by TEXES on NASA's Infrared Telescope Facility and Gemini-North will be presented and analysed. We find the magnitude and morphology of emission, and thus the thermal structure and chemistry of the stratosphere, exhibit both a short-term (daily) and longer-term (> 1 year) variability. On timescales of days, we find the magnitude of CH_4 , C_2H_2 and C_2H_4 emission within the auroral region to be variable in accordance with the external solar wind dynamical pressure. Over longer timescales, retrieved 1-mbar temperatures in the northern auroral region indicate a net cooling over the 2014 to 2018 period, which we attribute to the overall decrease in solar activity following solar maximum in 2014 and the approaching solar minimum in 2020-2021.

1. Introduction

Jupiter's auroral regions exhibit enhanced mid-infrared CH_4 , C_2H_2 , C_2H_4 and C_2H_6 emission (e.g. [1, 2, 3]). This indicates auroral processes can modify the thermal structure and composition of the neutral stratosphere at pressures between 1 mbar and 1 μbar (or between ~ 250 km and 550 km above the 1-bar level). This altitude range of the atmosphere is not probed by the Juno spacecraft due to the lack of mid-infrared remote-sensing instrumentation. In addition, ~ 1.7 MeV electrons or ~ 30 MeV protons precipitate at the 1-mbar level, which is an energy range outside of Juno's particle and field instrumentation [4, 5]. Thus, in order to enhance the science return of the Juno mission, we have performed a series of Earth-based mid-infrared measurements during the approach phase of the mission and *perijove* flybys occurring every 53.5 days. In this work, we will present an analysis of TEXES (Texas Echelon Cross Echelle Spectrograph, [6]) spectra obtained on NASA's Infrared Telescope Facility and Gemini-North as well as COMICS

(Cooled Mid-Infrared Camera and Spectrograph, [7]) images on the Subaru telescope, which capture the variability of Jupiter's mid-infrared auroral emission on timescales of days to years.

2. Observations

Table 1: Details of the measurements.

	Subaru-COMICS	IRTF-TEXES	Gemini-TEXES
Type	Imaging	Spectroscopy	Spectroscopy
λ	7.8 (CH_4)	8.03 (CH_4) 10.53 (C_2H_4) 12.21 (C_2H_6) 13.70 (C_2H_2) 17.03 (H_2 S(1))	8.03 (CH_4) 10.53 (C_2H_4) 12.21 (C_2H_6) 13.70 (C_2H_2) 17.03 (H_2 S(1))
$\lambda/\Delta\lambda$	-	$60\text{-}85 \times 10^3$	$60\text{-}85 \times 10^3$
Spatial resolution	0.25"	0.7 - 1.4"	0.25 - 0.55"
Dates	Jan 11, 12, 13, 14, Feb 4, 5, May 17, 18, 19, 20 2017	Dec 10-11 2014 Apr 30-May 1 2016 Jan 17 2017 Jun 3, 4 2017 Jul 13 2017 Feb 8 2018	Mar 17, 18, 19 2017

3. Short-term variability

The cadence of Subaru-COMICS and Gemini-TEXES measurements highlight the daily variability of the mid-infrared auroral emission. For example, Subaru-COMICS measurements in the January 11-13 2017 period (Figure 1) demonstrate both the morphology and magnitude of the auroral CH_4 emission is variable on timescales of days. From January 11th 15:50 UT to January 12th 16:13 UT, there was a brightening of the southern auroral CH_4 emission, which coincided with a solar wind compression event. The northern auroral region was on the opposing hemisphere on January 11th and so we cannot tell whether it also brightened during this time range. However, on January 12th, during the solar wind compression, the northern auroral emission exhibited a duskside (eastern) brightening, which was not present the following night on January 13th 12:30 UT. A similar 'active

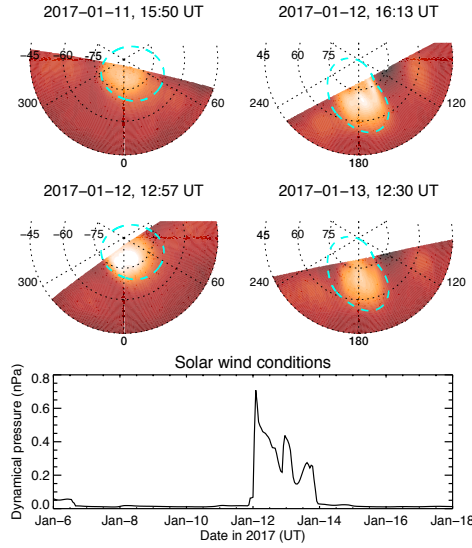


Figure 1: Southern (left column) and northern (right column) polar projections of 7.8-μm CH₄ emission from January 11-13 2017, as measured by Subaru-COMICS. The bottom plots show the predicted solar wind conditions [8] during this time period. The dashed, cyan lines mark the extent of the main ultraviolet oval emission [9].

duskside' morphology is exhibited in the ultraviolet auroral emission and is thought to be related to solar-wind induced reconnection in the nightside magnetopause [10].

4. Long-term variability

IRTF-TEXES measurements measured between December 2014 and February 2018 capture the longer-term variability of the auroral stratosphere. As shown in Figure 2, 1-mbar temperatures in the northern auroral region appeared invariant in time (within uncertainty) until mid-2017 and then significantly decreased by more than 10 K. Given that temperatures outside the northern auroral region in the same latitude band did not change significantly (outside of uncertainty), the observed temperature changes in the auroral region cannot be due to changes in the solar insolation alone. Instead, we believe the drop in 1-mbar temperatures in mid-2017 are a phase-lagged response of decreasing solar activity following solar maximum in 2014 towards the predicted solar minimum in 2020-2021. Oddly, the southern auroral region warmed by greater than 15 K from December 2014 to April 2016, independent of the north [11]. In mid-2017, the southern auroral region cooled back to similar temperatures as in December 2014 only to increase again 2-3 K by February 2018. This strongly suggests the northern and southern auroral regions behave very differently in time and exhibit

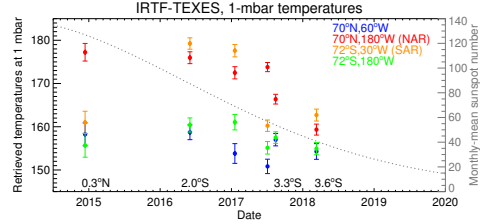


Figure 2: Retrieved temperatures at 1-mbar from IRTF-TEXES measurements between December 2014 and February 2018. Red and orange results indicate the northern and southern auroral regions, blue and green indicate non-auroral longitudes in the same latitude band for comparison. The grey, dotted line shows the monthly-mean sunspot number (<https://solarscience.msfc.nasa.gov/greenwch/>), according to the right-hand axis, as a proxy of longer-term solar activity.

differing responses to external magnetospheric and solar wind conditions, as is observed at other wavelengths [12].

5. Summary and conclusions

Jupiter's mid-infrared auroral emission exhibits both a short-term and long-term variability. Subaru-COMICS observations acquired over 2-3 days demonstrate that a component of the mid-infrared emission increases and decreases in accordance with the external solar wind pressure. Over longer timescales, a preliminary analysis of IRTF-TEXES measurements indicate 1-mbar temperatures in the northern auroral region exhibited a net cooling of more than 10 K, which we believe to be a phase-lagged response of decreasing longer-term solar activity following solar maximum in 2014. The northern auroral region appears to behave independently of the southern auroral region and vice-versa.

References

- [1] J. Caldwell, F. C. Gillett and A. K. Tokunaga, 1980, *Icarus* 44, 667-675.
- [2] T. Kostiuk et al., 1993, *JGR* 98:18823.
- [3] Sinclair et al., 2017a, *Icarus* 292, 182-207.
- [4] Mauk et al., 2017, *Space Science Reviews* 213 (1-4), 289-346.
- [5] McComas et al., 2017, *Space Science Reviews* 213 (1-4), 547-643.
- [6] Lacy et al., 2002, *PASP* 114:153-168.
- [7] Kataza et al., 2000, *Proc. SPIE Vol. 4008*, p. 1144-1152.
- [8] Tao et al., 2005, *JGR: Space Physics*, 110 (A11), 2005.
- [9] Bonfond et al., 2012, *GRL* 39:L01105, 2012.
- [10] Nichols et al., 2017, *GRL* 44(15), 7643-7652.
- [11] Sinclair et al., 2017b, *GRL* 44, 5345-5354.
- [12] Dunn et al., 2017, *Nature Astronomy* 1, 758-764.

Jupiter's magnetic field & Io-related decameter radiation

Y. M. Martos (1,2), J.E.P. Connerney (1,3), S. Kotsiaros (1,2) and M. Imai (4)

(1) NASA Goddard Space Flight Center, Greenbelt, USA, (2) University of Maryland, College Park, USA, (3) Space Research Corporation, Annapolis, USA, (4) The University of Iowa, Iowa City, USA, (yasmina.martos@nasa.gov)

Abstract

The Io-dependent radio emissions from Jupiter ought to originate along magnetic field lines linking Io to the Jovian ionosphere. If these emissions occur at or below the electron gyrofrequency, they ought to be limited in frequency extent by the magnetic field magnitude at the foot of the Io Flux Tube (IFT), a subject of much interest since the 1980's. The lack of agreement between the frequency extent of Io-related decameter radiation and those predicted by Jovian magnetic field models has been hotly debated. In this study we show how the newly proposed magnetic field model (JRM09) can explained these radio emissions. Additionally, the beaming angle of the hollow cone of emission and the altitude of the generation of the decameter radio emissions are estimated and discussed.

1. Main text

Two main forms of decametric radio emissions are observed from Jupiter: S bursts and L emissions. The first one is very brief (ms) and intense (S bursts) comprising very discrete spectral components with very narrow bandwidth. The second emission is smoother, with longer duration (seconds) with a broad frequency bandwidth (L emissions). Statistical studies of the peak frequencies of the Io-related decameter radio emissions compared with the electron cyclotron frequencies at the foot of the Io field line have been performed by several authors (e.g. [4,6]), reporting a delay of up to 70° between the two. Different hypotheses have been proposed to explain the delay including an Alfvén-wave propagation through the Io plasma torus and the existence of an extended magnetotail for Io [4].

In addition, other options to reconcile the observations with a Jovian magnetic model include obtaining and constraining a magnetic model itself

using the peak frequencies of the radio emission observations (e.g. VIPAL model [5]) as a constraint on the surface magnetic field magnitude. However, this kind of constraint may provide good agreement in specific locations where the constraint is applied but such models may lead to very inaccurate estimates of the field in other regions of Jupiter (e.g., regions lacking either direct observations or constraints).

Very recently, a new magnetic field model of Jupiter's planetary field has been proposed, JRM09 [2], using observations from the Juno spacecraft's first nine orbits. Juno is currently orbiting Jupiter every 53 days with the intention of collecting a dense global net of potential field data (among others) at close radial distances never measured before [3].

The JRM09 model represents a partial solution to a degree 20 spherical harmonic expansion, yielding coefficients through degree 10 with adequate resolution. This high-resolution model yields magnetic field magnitudes of up to 20 G along the IFT footprint, substantially higher than previous models. Using the JRM09 field model, we compare the observed frequency peak of Io-related decameter radiation with the gyrofrequency (f_c (MHz) = $2.8 \cdot B$ (Gauss)) at the foot of the Io field line predicted by the new model (Figure 1). This shows that all the L emissions and the S bursts can be explained by the cyclotron frequencies, except possibly for the few observations located around 60° Io longitude where the field magnitude drops precipitously.

We note with interest that the observed maximum frequency of emission appears offset from that appropriate to the IFT foot, either vertically, or equivalently, in system 3 longitude. This may be related to a combination of lead angle, emission cone angle, and altitude of emission, to be determined.

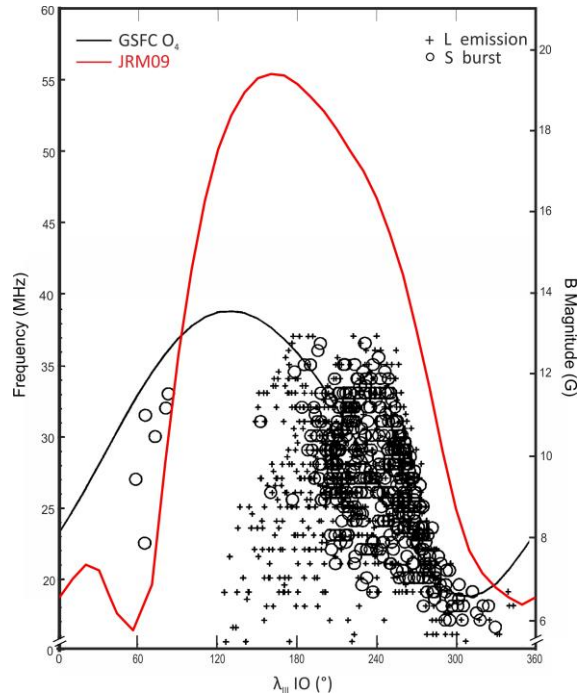


Figure 1. Comparison of the peak frequencies of the Io-related decameter radiation (S bursts and L emissions) and the gyrofrequency at the foot of the Io field line predicted by the GSFC O₄ [1] and JRM09 [2] magnetic field models.

Acknowledgements

This research is supported by the Juno Project under NASA grant NNM06AAa75c to SWRI and NASA grant NNN12AA01C to JPL/Caltech. The Juno mission is part of the New Frontiers Program managed at NASA's Marshall Space Flight Center in Huntsville, Alabama.

References

- [1] Acuña, M. H., Kenneth W. Behannon, and J. E. P. Connerney, Jupiter's magnetic field and magnetosphere, *Physics of the jovian magnetosphere*: 1-50, 1983.
- [2] Connerney, J. E. P., et al., A New Model of Jupiter's Magnetic Field From Juno's First Nine Orbits, *Geophysical Research Letters* 45.6: 2590-2596, 2018.
- [3] Connerney, J. E. P., et al., The Juno magnetic field investigation, *Space Science Reviews* 213.1-4, 39-138, 2017.
- [4] Genova, F., and Calvert, W., The source location of Jovian millisecond radio bursts with respect to Jupiter's magnetic field, *Journal of Geophysical Research: Space Physics* 93.A2, 979-986, 1988.
- [5] Hess, S. L. G., Bonfond, B., Zarka, P., and Grodent, D., Model of the Jovian magnetic field topology constrained by the Io auroral emissions. *Journal of Geophysical Research: Space Physics*, 116(A5), 2011.
- [6] Marques, M. S., Zarka, P., Echer, E., Ryabov, V. B., Alves, M. V., Denis, L., and Coffre, A., Statistical analysis of 26 yr of observations of decametric radio emissions from Jupiter, *Astronomy & Astrophysics* 604, A17, 2017.

Jovian broadband kilometric radio sources correlated with the ultraviolet main oval as viewed from Juno

M. Imai (1), T. K. Greathouse (2), G. R. Gladstone (2), W. S. Kurth (1), C. K. Louis (3), G. B. Hospodarsky (1), P. Zarka (3), S. J. Bolton (2), J. E. P. Connerney (4), and S. M. Levin (5)
(1) University of Iowa, Iowa City, Iowa, USA, (2) Southwest Research Institute, San Antonio, Texas, USA, (3) LESIA, CNRS, Observatoire de Paris, Meudon, France, (4) NASA Goddard Space Flight Center, Greenbelt, Maryland, USA, (5) Jet Propulsion Laboratory, California Institute of Technology, Pasadena, California, USA (masafumi-imai@uiowa.edu / Fax:+1-319-335-1753)

Abstract

Since 5 July, 2016, the Juno spacecraft has toured Jupiter in a 53-day eccentric polar orbit. During each perijove survey, Juno has monitored complex auroral activity in radio and ultraviolet (UV) wavelengths by means of the radio and plasma wave instrument (Waves) [1] and the UV spectrograph instrument (Juno-UVS) [2]. Waves uses three onboard receivers to monitor the electric fields of waves from 50 Hz to 41 MHz with an electric dipole antenna and the magnetic fields of waves from 50 Hz to 20 kHz with a magnetic search coil sensor. Juno-UVS is designed to image and obtain spectra in a wavelength range from 68 to 210 nm with a 4 cm by 4 cm aperture, where the field of view of a flat scan mirror is adjustable within $\pm 30^\circ$ with respect to the Juno's spin plane. In contrast to continuous Jovian radio monitoring from Waves, Juno-UVS data is typically collected for a time span of ~ 10 hours centered at perijove. We have analyzed simultaneous Waves and Juno-UVS data obtained for time spans of 2 hours over both hemispheres during perijoves 4 (PJ4) on 2 February, PJ5 on 27 March, and PJ6 on 19 May, 2017. For all six time periods, Juno traversed magnetic field lines connecting to the UV main oval, matching the estimates of the Jovian broadband kilometric (bKOM) radio source footprints. The localized bKOM radio sources for the PJ4 north pass map to magnetic field lines extending from 10 to 12 Jovian radii (R_J) at the equator, whereas the extended bKOM radio sources for the other passes are on field lines extending to 20–60 R_J . We find that the latter bKOM radio sources are stable in the presence of variations in UV brightness. In this paper, we present a summary of simultaneous observations of Jovian bKOM radio emissions and UV aurora images taken from Juno.

References

- [1] Kurth, W. S., Hospodarsky, G. B., Kirchner, D. L., Mokrzycki, B. T., Averkamp, T. F., Robison, W. T., Piker, C. W., Sampl, M. and Zarka, P.: The Juno Waves Investigation, *Space Sci. Rev.*, Vol. 213, pp. 347–392, 2017.
- [2] Gladstone, G. R., et al.: The Ultraviolet Spectrograph on NASA's Juno Mission, *Space Sci. Rev.*, Vol. 213, pp. 447–473, 2014.

Jupiter's magnetic field morphology: Implications for the dynamo

Kimberly Moore (1), Rakesh Yadav (1) Laura Kulowski (1) Hao Cao (1) Jeremy Bloxham (1) John E. P. Connerney (2,3) Stavros Kotsiaros (2,4) John L. Jorgensen (5) Jose M. G. Merayo (5) David J Stevenson (6) Scott J. Bolton (7) and Stevin M. Levin (8)

(1) Department of Earth & Planetary Sciences, Harvard University, USA (kimberlymoore@g.harvard.edu) (2) NASA Goddard Spaceflight Center, USA (3) Space Research Corporation, Maryland, USA (4) University of Maryland, College Park, USA (5) National Space Institute, Technical University of Denmark, Kongens Lyngby, Denmark (6) Division of Geological and Planetary Sciences, California Institute of Technology, USA (7) Southwest Research Institute, San Antonio, Texas, USA (8) Jet Propulsion Laboratory, California Institute of Technology, USA

Abstract

Now that the NASA Juno Mission has collected magnetometer data from over eight evenly spaced pole-to-pole passes, we can examine Jupiter's global magnetic morphology. The two hemispheres are distinctly different, with a strong localized band of flux in the north, compared to a smoother and weaker dipolar flux in the southern hemisphere. Low flux over the North Pole, and a large spot of equatorial flux (the Great Blue Spot) are also apparent. We discuss the implications of these observed features for Jupiter's dynamo and interior.

1. Introduction

As of late 2017, the NASA Juno Mission [1, 2] has collected magnetic field data from 8 orbital passes. Due to Juno's near polar orbit around Jupiter, the roughly equal longitudinal spacing of the orbits and, most importantly, the close approach distance to Jupiter's dynamo (within about 20% of the planetary radius) these data provide an unprecedented view of an active dynamo. The initial results reveal an unexpected field morphology [3, 8].

2. Field Morphology

Before data collected by the NASA Juno Mission, models of Jupiter's magnetic field [4, 9] closely resembled Earth's field—a strong, tilted dipole. Juno data might have been expected to reveal progressively smaller-scale structure in the field, with the same overall structure. However, the morphology we now see is striking and unexpected. Figure 1 shows maps of Jupiter's magnetic field from a model, JRM09 [3]. Several distinctive features are visible,

with important dynamo implications [8]. We describe them below.

First, at the top of the nominal dynamo region, we see large-scale field organization. Flux emerges from Jupiter's northern hemisphere in a relatively narrow band around 45 degrees N, and stretches across about 270 degrees of longitude. In contrast, in the southern hemisphere we see flux re-enter over a large diffuse region, in which the maximum radial flux is only a third of that seen in the northern hemisphere. Elsewhere (except near the equator), the radial field is much weaker. We see strong evidence of locally reduced (and possibly reversed) flux near the North Pole (see also [5, 6, 7]).

At the equator we see an extraordinarily intense and localized spot of negative flux (the Great Blue Spot, first seen by [7]), in which the radial flux is three times stronger than any other negatively signed flux. While the JRM09 model accounts for Jupiter's magnetodisc field, we note there may be additional unmodeled auroral currents or external field effects. However, these are unlikely to affect the overall morphology described here.

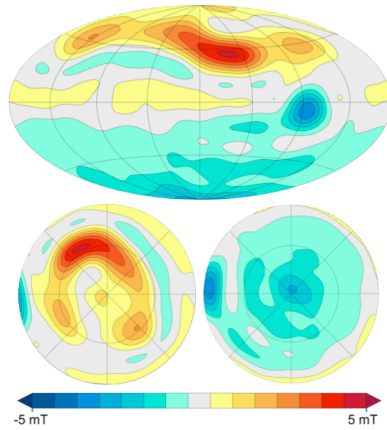


Figure 1: This figure shows the radial magnetic field from the degree 10 spherical harmonic model JRM09 at 0.85 RJ (with Jupiter radius $R_J = 71492\text{km}$). The upper map is centered on 180° W (System III 1965 coordinates). The left (right) maps show the northern (southern) hemisphere in a Lambert azimuthal equal-area projections.

3. Conclusions

In our presentation, we discuss the initial dynamo implications of Jupiter's magnetic field morphology. However, the full 32 orbits planned for Juno will be necessary to reveal these features more fully.

Acknowledgements

This research was supported by the NASA Juno Mission, the National Defense Science & Engineering Graduate Fellowship (KM), and the NSF Graduate Fellowship (LK).

References

- [1] Bolton, S. J., et al: Jupiter's atmosphere and deep interior: The initial pole-to-pole passes with the Juno spacecraft, *Science*, Vol 356, Issue 6340, pp. 821-825, 2017.
- [2] Connerney, J. E. P. et al.: The Juno magnetic field investigation, *Space Science Reviews*, Vol 213, pp.39-139, 2017.
- [3] Connerney, J. E. P., Kotsiaros, S., Oliverson, R. J., Espley, J. R., Joergensen, J. L., Joergensen, P. S., Merayo, J. M. G., Hecceg, M., Bloxham, J., Moore, K. M., Bolton, S. J., and Levin, S. M.: A new model of Jupiter's magnetic field from Juno's first nine orbits, *Geophysical Research Letters*, Vol 45, 2590-2596, 2018.
- [4] Connerney, J. E. P., Acuña, M. H., Ness, N. F., and Satoh, T: New models of Jupiter's magnetic field constrained by the Io flux tube footprint, *Journal of Geophysical Research: Space Physics*, Vol 103, 11929-11939, 1998.
- [5] Grodent, D., Bonfond, B., Gerard, J.-C., Radioti, A., Gustin, J., Clarke, J. T., Nichols, J., and Connerney, J. E. P.: Auroral evidence of a localized magnetic anomaly in Jupiter's northern hemisphere, *Journal of Geophysical Research*, Vol 113, A09201, 2008.
- [6] Hess, S. L. G., Bonfond, B., Zarka, P., and Grodent, D: Model of the Jovian magnetic field topology constrained by the Io auroral emissions, *Journal of Geophysical Research: Space Physics*, Vol 116, A05217, 2011.
- [7] Moore, K. M., Bloxham, J., Connerney, J. E. P., Jorgensen, J. L., and Merayo, J. M. G: The analysis of initial Juno magnetometer data using a sparse magnetic field representation, *Geophysical Research Letters*, Vol 44, 2017GL073133, 2017.
- [8] Moore et al., Jupiter's magnetic field morphology: Implications for the dynamo, In review.
- [9] Ridley, V. A. and Holme, R: Modeling the Jovian magnetic field and its secular variation using all available magnetic field observations, *Journal of Geophysical Research: Planets*, Vol 121, 2015JE004951, 2016.

Jupiter's high-latitude hazes as mapped by JunoCam

J.H. Rogers (1), G. Eichstädt (2), C. J. Hansen (4), G. S. Orton (5), T.W. Momary (5), F. Tabataba-Vakili (5), M.A. Caplinger (6), M.A. Ravine (6), C. Go (7), A. Casely (7), M. Jacquesson (3).

(1) British Astronomical Association, London, UK; (2) Independent scholar, Stuttgart, Germany; (3) JUPOS team; (4) Planetary Science Institute, Tucson, Arizona, USA; (5) Jet Propulsion Laboratory, California Institute of Technology, Pasadena, California, USA; (6) Malin Space Science Systems, San Diego, California, USA; (7) Independent observers. [\[jrogers11@btinternet.com\]](mailto:jrogers11@btinternet.com)

Abstract

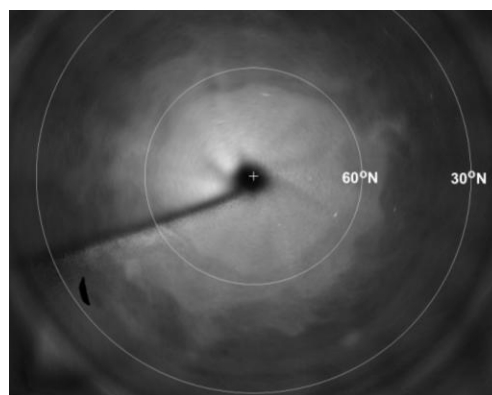
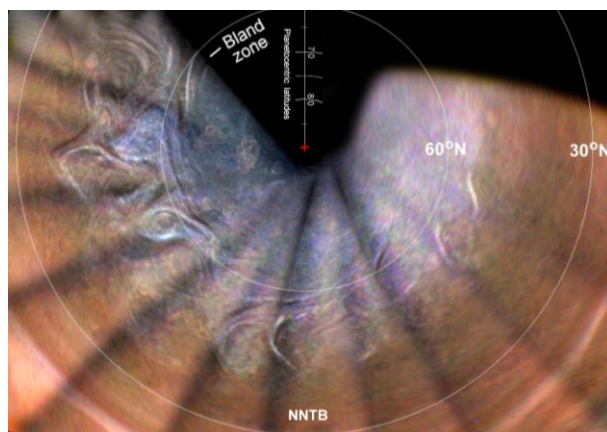
The JunoCam instrument on the Juno spacecraft takes images of Jupiter's polar regions at every perijove and reveals elaborate patterns of haze bands. In visible-colour images, they include white bands, dark brown bands, and 'rainbow bands'. All are seen mainly near the terminator, but brown bands are sometimes also seen under full sunlight. Some of them are also visible in methane-band images (889 nm, detecting reflected sunlight from high-altitude aerosols), but the relationship is complex. In addition to the localised bands, the polar regions are covered with the well-known North and South Polar Hoods (NPH, SPH), which appear bluish (but not noticeably opaque) in JunoCam's visible-colour images, and bright in methane-band images. Here we describe these patterns with particular reference to Perijove 12 (PJ12) on 2018 April 1. These maps show very clearly the high-latitude haze patterns previously seen at lower resolution from Hubble and Cassini and in ground-based infrared images. The main outlines of these haze features can also be detected in the best amateur methane-band images from 2018.

Northern hemisphere

In the north, the most noticeable haze bands are long linear bands in what we call the Bland Zone (roughly lying between two prograde jets at 61 and 66°N, planetocentric). These were seen at PJ1 [ref.1]; they are slightly oblique, and often consist of adjacent white and brown bands. There are few visible haze bands at higher latitudes, where the NPH is densest. But at <61°N, there are often conspicuous bands at various angles near the terminator.

PJ12 was special because Juno inbound viewed the planet at higher phase angles than before, and the images showed mainly the high-altitude hazes all across the crescent. [Figure 1](#) is the first detailed map of the northern hazes. The map shows the NPH extending down to the Bland Zone, where the usual linear bands can be seen. From there, similarly bluish-white bands and arcs extend to the south in huge waves and swirls, covering several domains down to ~31°N (the N2 jet).

[Fig.2](#) is a methane-band map for comparison. It shows multiple edges to the methane-bright NPH, which correspond to waves and swirls in [Fig.1](#).



Figures 1 & 2. Northern hazes: composites of polar projection maps of the PJ12 inbound images, all at high phase angle. **Fig.1** (RGB): The white features are high-altitude hazes. **Fig. 2** (methane band).

South of 61°N, these hazes do not obviously match the known zonal wind profile, but they may be influenced by it. We suggest that they may arise in the N4 and N5 domains, and spread northwards and southwards until entrained by the next or next-but-

one prograde jet. The N4 and N5 domains are largely filled with ‘folded filamentary regions’ which generate the most frequent lightning strikes on the planet, and could be generating the hazes.

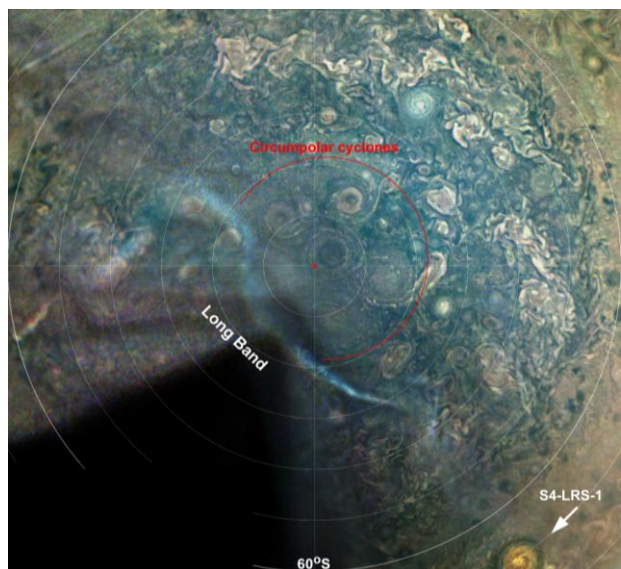
Southern hemisphere

Fig.3 shows a composite map of south polar haze bands. One conspicuous long haze band has been present in similar position at every perijove since PJ4. This arc-shaped ‘Long Band’ appears to be structurally related to the pentagon of cyclones that surrounds the south pole [ref.2]. It is often composed of adjacent brown and white bands, the latter often being ‘rainbow bands’ near the terminator (see below). North of the SPH, narrower bands are often seen in the S5 and S4 domains [not shown here].

Fig.4 is a methane-band map for comparison. It shows the wave system around the edge of the methane-bright SPH (= S6 jet). The Long Band is seen as a boundary within the SPH.

Discussion

The properties of these haze bands are complex. White and brown bands often form tight bundles, and sometimes a band appears white when illuminated from one side and dark when illuminated from the other (i.e., diurnal variation). *White bands* are seen mainly near the terminator, sometimes projecting across it, demonstrating their high altitude [ref.1], above the polar hoods; however they are not always strongly methane-bright. Sometimes they are



‘rainbow bands’, i.e. bright bluish on one side, usually sun-facing (possibly due to wavelength-dependent scattering in the thin outer fringe of the band) and reddish on the other, usually shadowed side (due to any of the following explanations for brown bands).

Brown bands could be explained by some or all of the following hypotheses:

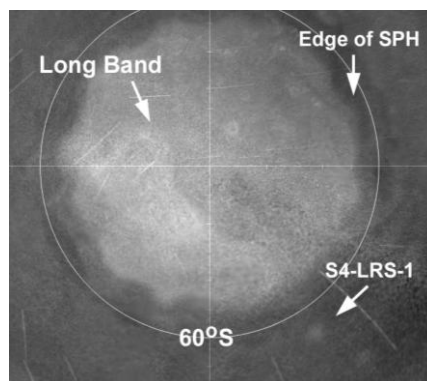
- (1) They may be shadows cast by the white bands, with diffusely scattered red light;
- (2) They may be clear lanes within the diffuse bluish-white polar hoods;
- (3) They may be bands of brown aerosols;
- (4) As brown bands are usually adjacent to white bands, these may be waves of alternating thinner and thicker haze, and/or, waves in which particles are tilted at slightly different angles.

Acknowledgements

This research was largely funded by NASA through the Juno project. A portion of this was distributed to the Jet Propulsion Laboratory, California Institute of Technology.

References

- [1] Orton GS, *et al.* (2017) ‘The first close-up images of Jupiter’s polar regions: Results from the Juno mission JunoCam instrument.’ GRL 44, 4599–4606.
- [2] Adriani A, Mura A, Orton G, Hansen C, Altieri F, Moriconi ML, Rogers J, Eichstädt G, *et al.* (2018) ‘Clusters of Cyclones Encircling Jupiter’s Poles.’ Nature 555, 216-219.



Figures 3 & 4: Composite polar projection maps of the PJ12 images over the south pole and outbound.

Fig.3 (left: RGB): In the lower and left-hand sides, it emphasises the regions near the terminator where haze bands (bright or dark) are seen.

Fig.4 (top right: methane band).

Field aligned currents associated with Jupiter's auroras

S. Kotsiaros (1, 2), J. E. P. Connerney (1, 3), G. R. Gladstone (4), W. S. Kurth (5), G. Clark (6), F. Allegrini (4, 9), B. H. Mauk (6), T. K. Greathouse (4), E. J. Bunce (7), Y. M. Martos (1, 2), S. J. Bolton (4), S. M. Levin (8)

(1) NASA Goddard Space Flight Center, Greenbelt, USA, (2) University of Maryland College Park, College Park, Maryland, USA, (3) Space Research Corporation, Annapolis, USA, (4) Southwest Research Institute, San Antonio, TX, USA, (5) Department of Physics and Astronomy University of Iowa, Iowa City, IA, USA, (6) Johns Hopkins University Applied Physics Lab, Laurel, Maryland, USA, (7) Department of Physics and Astronomy, University of Leicester, Leicester, UK, (8) Jet Propulsion Laboratory (JPL), Pasadena, CA, USA, (9) Department of Physics and Astronomy, University of Texas at San Antonio, San Antonio, Texas, USA.

Abstract

Jupiter's aurorae are huge in size, and hundreds of times more energetic than those on Earth. Therefore, intense field-aligned currents accompanied by large magnetic field perturbations were expected, similarly to the Earth, along field lines rooted in the main auroral oval. Here, we present observations of magnetic field perturbations due to field-aligned currents. The nature and the characteristics of the perturbations and consequently of the field-aligned currents are discussed.

1. Introduction

The Juno spacecraft has been orbiting Jupiter since July 4, 2016. It has performed 12 periapsis passes and continues sampling the Jovian environment close up (to 1.06 Jovian radii, R_J) extending to the outer reaches of the Jovian magnetosphere[1]. Juno's polar orbit makes it possible to acquire for the first time direct observations of the jovian magnetosphere and auroral emissions above the poles.

2. Magnetic field perturbations

Juno's vector magnetic field measurements during the first traversal over Jupiter's polar regions revealed a puzzling situation: Jupiter did not show intense field-aligned currents associated with the main aurora. Specifically, strong magnetic perturbations that should have resulted from the expected strong sheets of electric currents were not evident[1]. An extended analysis of Juno's magnetic field observations over Jupiter's polar regions has now revealed that the magnetic field perturbations associated with auroral field aligned currents are weak (maximum up to ± 400 nT) and are therefore masked by the strong internal field of Jupiter

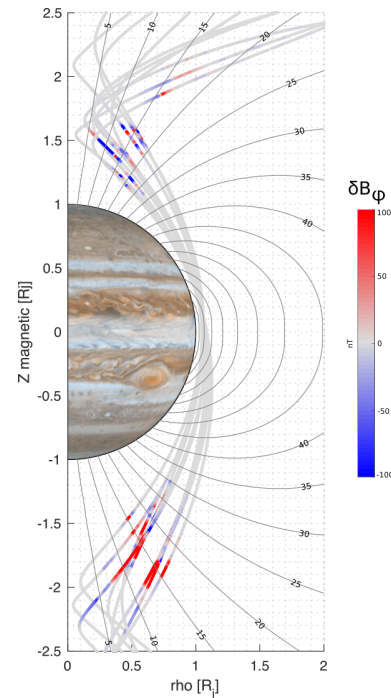


Figure 1: Magnetic field perturbations in the B_ϕ component obtained from Juno's magnetic field observations after removing estimates from JRM09 model[2]. The fiducial field lines, computed from JRM09 model with their associated L-shell values are also plotted.

(typically about 2 Gauss where the perturbations occur). The magnetic field perturbations are extracted from the magnetic field vector data after removing estimates of the internal field from JRM09[2] along Juno's trajectory as well as removing remaining non-linear trends by fitting a smoothing spline based on a penalized least squares method[3]. Figure 1 shows the

resulting magnetic field perturbations in the B_ϕ component for each periapsis pass. The fiducial field lines, computed from JRM09 model with their associated L-shell values are also plotted. The perturbations are found in transit across field lines rooted to the main aurora. A strong asymmetry between the field perturbations over the north and south polar regions is also evident. Specifically, the field perturbations over the north appear more dispersed showing dynamic filamentary structures whereas the perturbations over the south tend to get organized in two main regions of positive and negative δB_ϕ suggesting coherent sheets of field aligned currents.

3. Summary and Conclusions

Jupiter presents the most powerful aurorae in our solar system. Images of intense aurorae have been captured by Juno’s ultraviolet and infrared imaging spectrographs. Surprisingly, the magnetic field perturbations associated with Jupiter’s auroral field aligned currents are weaker than expected. Unlike Earth, Jupiter’s field-aligned currents linked with the northern aurora do not seem to flow in organized regions of clearly defined parallel sheets but show dynamic filamentary structures.

4. Acknowledgements

This research is supported by the Juno Project under NASA grant NNM06AA75c to SWRI and NASA grant NNN12AA01C to JPL/Caltech. The Juno mission is part of the New Frontiers Program managed at NASA’s Marshall Space Flight Center in Huntsville, Alabama.

References

- [1] Connerney, J. E. P., Adriani, A., Allegrini, F., Bagenal, F., Bolton, S. J., Bonfond, B., Cowley, S. W. H., Gerard, J. C., Gladstone, G. R., Grodent, D., Hospodarsky, G., Jorgensen, J. L., Kurth, W. S., Levin, S. M., Mauk, B., McComas, D. J., Mura, A., Paranicas, C., Smith, E. J., Thorne, R. M., Valek, P., Waite, J.,: Jupiter’s magnetosphere and aurorae observed by the Juno spacecraft during its first polar orbits, *Science*, Vol. 356, pp. 826-832, 2017.
- [2] J. E. P. Connerney, S. Kotsiaros, R. J. Oliverson, J. R. Espley, J. L. Joergensen, P. S. Joergensen, J. M. G. Merayo, M. Hecceg, J. Bloxham, K. M. Moore, S. J. Bolton, S. M. Levin: A New Model of Jupiter’s Magnetic Field From Juno’s First Nine Orbits, *Geophysical Research Letters*, Vol. 45, pp. 2590-2596, 2018.
- [3] D. Garcia.: Robust smoothing of gridded data in one and higher dimensions with missing values, *Comput Stat Data Anal*, Vol. 54(4), pp. 1167–1178, 2010.

First hints on tropospheric composition at Jupiter's polar regions from JIRAM-Juno data

Davide Grassi (1), Alberto Adriani (1) Alessandro Mura (1) Scott Bolton (2) and the JIRAM Juno team
 (1) IAPS-INAF, Roma, Italy (2) SwRI, San Antonio, USA (davide.grassi@iaps.inaf.it)

Abstract

1. Introduction

The Jupiter InfraRed Auroral Mapper (JIRAM) instrument on the NASA Juno spacecraft hosts an imager operating around $5\ \mu\text{m}$ and a spectrometer operating between 2 and $5\ \mu\text{m}$, with a spectral resolution of about $15\ \text{nm}$. The imager and the spectrometer have a spatial resolution of $250\ \mu\text{rad}$ and are operated simultaneously. While most regions of Jupiter are usually affected by a thick cloud coverage, clearance areas (with cloud total opacities < 1 in the $5\ \mu\text{m}$ range) exist at specific locations, notably the hot spots frequently observed between the equatorial zone and the north equatorial belt [4]. In these conditions, JIRAM spectra are sensitive to the contents of ammonia, water vapour, phosphine and – in lesser degree – germane, at the approximate levels between 2 and $3\ \text{bar}$ [5], well below the Jupiter tropopause.

2. Materials

While tropospheric composition in hot spots and in extended regions at Jupiter's low and intermediate latitudes has been investigated by a number of authors on the basis of spacecraft and ground telescope data (e.g. [2], [3]), no study has yet covered polar regions. However, during the Juno's fourth periapsis (February 2nd 2017) the JIRAM instrument has eventually acquired extensive observations over both poles. The JIRAM imager revealed a surprisingly regular pattern of nine large cyclones on the north pole and – similarly surprising – six more cyclones on the south pole [1].

In this work, we present a first attempt to map tropospheric composition at Jupiter's polar regions from JIRAM spectral data. Analysis was performed according the methods presented in [5] and limited to

spectra with lower emission angle (to limit retrieval uncertainties) and higher signal (retrievals are not possible in regions with thick cloud coverage).

3. Results

Example maps are presented in figures 1 and 2.

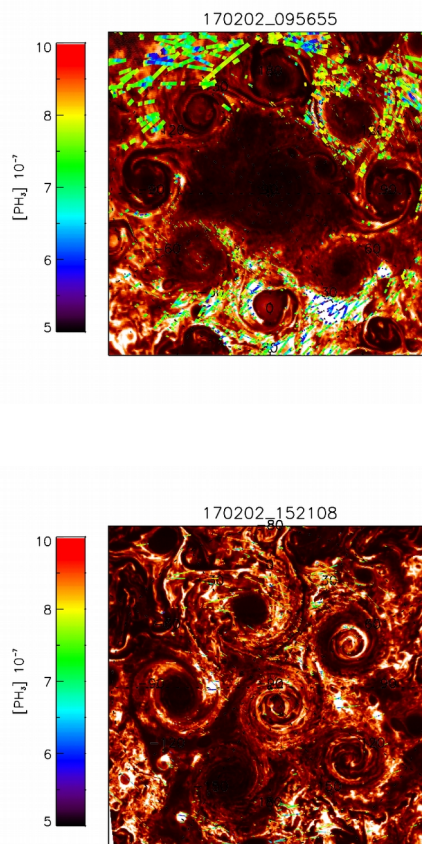


Figure 1: Phosphine content over the two polar regions

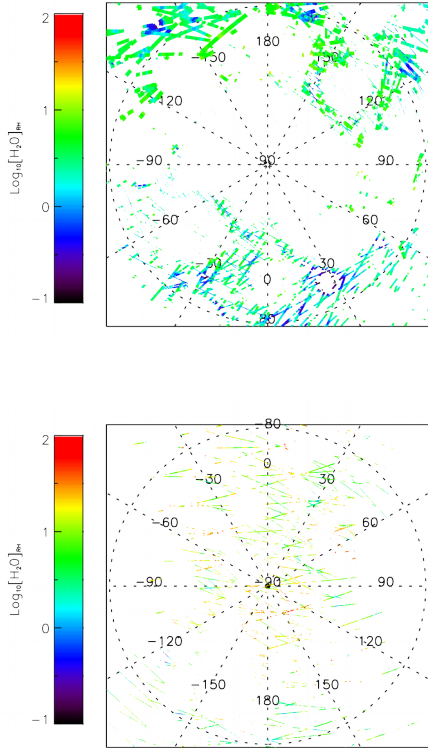


Figure 2: Comparison of water content over the two poles.

Brighter (clear) regions are found to be considerably depleted in disequilibrium species (PH_3 and GeH_4) once compared against darker (moderately cloudy) ones, suggesting effective suppression of vertical upwelling. Concentration contrasts between bright and dark area appear stronger over the northern pole. Contents of condensable species (H_2O and NH_3) are enhanced over the south pole, possibly associated with smaller overall opacity of cyclones there.

Acknowledgements

This work was supported by the Italian Space Agency through ASI-INAF contract I/010/10/0 and 2014-050-R.0. The JIRAM instrument has been developed by Leonardo at the Officine Galileo - Campi Bisenzio site. The JIRAM instrument was conceived and brought to reality by our late collaborator and institute director Dr. Angioletta Coradini (1946-2011).

References

- [1] Adriani, A. et al., *Geometric cyclonic patterns in Jovian Polar Regions*, Nature, 555, doi:10.1038/nature25491, 2018
- [2] Giles, R.S., et al. *Cloud structure and composition of Jupiter's troposphere from 5-m Cassini VIMS spectroscopy*, Icarus, 257, 457-470, doi:10.1016/j.icarus.2015.05.030, 2015
- [3] Giles, R.S., et al. *Latitudinal variability in Jupiter's tropospheric disequilibrium species: GeH_4 , AsH_3 and PH_3* , Icarus, 289, doi:10.1016/j.icarus.2016.10.023, 2017
- [4] Grassi, D., et al., *Preliminary results on the composition of Jupiter's troposphere in hot spot regions from the JIRAM/Juno instrument*, Geophys. Res. Lett., 44, doi:10.1002/2017GL072841, 2017
- [5] Grassi, D., et al., *Analysis of IR-bright regions of Jupiter in JIRAM-Juno data: Methods and validation of algorithms*, Journal of Quantitative Spectroscopy and Radiative Transfer, 202, doi:10.1016/j.jqsrt.2017.08.008, 2017.

Juno/JIRAM infrared observations of Jupiter: results of the first two years

A. Mura¹, A. Adriani¹, J. E. P. Connerney², S. Bolton³, F. Altieri¹, B.M. Dinelli⁴, M.L. Moriconi⁴, M. Amoroso⁵, A. Cicchetti¹, F. Fabiano², G. Filacchione¹, D. Grassi¹, A. Migliorini¹, R. Noschese¹, A. Olivieri⁵, G. Piccioni¹, C. Plainaki⁵, G. Sindoni¹, R. Sordini¹, F. Tosi¹, D. Turrini¹

¹ *National Institute for Astrophysics, Italy,* ² *Southwest Research Institute, United States,* ³ *NASA Goddard Space Flight Center, United States,* ⁴ *Consiglio Nazionale delle Ricerche, Italy,* ⁵ *ASI, Italy,*

Abstract

JIRAM, the Jovian InfraRed Auroral Mapper on board NASA/Juno mission, is an infrared camera and a spectrometer working in the infrared spectral range 2-5 μm . The primary scientific objectives of the instrument are the study of the infrared aurora emitted from H_3^+ excited by electron precipitation, and the study of the concentrations of atmospheric compounds like water, ammonia and phosphine. There are present in the Jupiter troposphere and, in particular, in the hot spots and below the cloud deck. In addition, JIRAM could study of Jupiter's clouds and the dynamics of the atmosphere, the galilean moons.

The instrument was able to get its observations during the PJ1 and from PJ4 to PJ 14 passes, resulting in an almost complete coverage of both the auroral and the atmospheric emission from the planet. Here we present a highlights from the results obtained from those observations.

Properties of lightning whistlers observed in the topside ionosphere of Jupiter

O. Santolik (1,2), I. Kolmasova (1,2), M. Imai (3), D. A. Gurnett (3), G. B. Hospodarsky (3), W. S. Kurth (3), and S. J. Bolton (4)

(1) Department of Space Physics, IAP CAS, Prague, Czechia, (2) Charles University, Prague, Czechia, (3) University of Iowa, Iowa City, IA, USA, (4) Southwest Research Institute, San Antonio, TX USA

Abstract

Short impulsive signals from lightning in Jovian atmosphere are dispersed by their passage through the plasma environment of the planet into the characteristic form of whistlers. Electromagnetic measurements of the Juno Waves instrument allow us to collect the largest existing set of lightning detections and to observe different spectral forms of whistlers at short time scales. Comparison of their observed frequency-time structure with calculations of their frequency dependent group delays allows us to analyze parameters of the low-density plasma in the topside ionosphere of Jupiter.

1. Introduction

Lightning generated electromagnetic waves were discovered in the dense plasma of Io torus by Voyager 1 [1]. They were dispersed by their passage through the plasma medium into the form of whistlers at time scales of several seconds and at frequencies of several kHz.

The unique polar orbit of the Juno spacecraft [2] allows us to observe “rapid” whistlers in the topside ionosphere very close to Jupiter [3]. As their path through the dense plasma is short, the accumulated dispersion is low, and the time scales of these whistlers decrease to only several units to tens of milliseconds.

2. Statistics of detections

The Juno Waves instrument [4] observed 1627 “rapid” whistlers during the initial 8 close approaches to the planet at radial distances below 5 Jovian radii [3]. This outnumbers all previous lightning data sets from Jupiter. Voyager 1 observed 167 whistlers,

followed by 434 optical lightning detections from Voyager 1 and 2, Galileo, Cassini, New Horizons, and by 377 Juno MWR “sferics” at 600 MHz [5].

A maximum rate of more than 4 whistlers per second has been observed by Juno. Statistics of whistler rates give us average values of more than 1 whistler/s between $+40^\circ$ and $+55^\circ$ magnetic latitude in the northern hemisphere and more than 0.5 whistler/s between -65° and -50° in the southern hemisphere.

A rough categorization according to the observed dispersion properties provides us with two dispersion classes: Class 1 with a difference of propagation delays at 2 and 5 kHz of less than 5 ms, and Class with larger differences [3]. However, the observed time-frequency spectrograms of Jovian whistlers can be more complex, exhibiting signs similar to terrestrial ion whistlers, as well as sudden “hook” and “flag” signatures in whistler traces.

Analysis of the relative phase and coherency between the electric and magnetic field signals recorded by Juno Waves allows us to determine that these waves propagate outward from the planet.

3. Calculations of the propagation delay

We use the VIP4 magnetic field [6] model recalibrated to the local measurements of the magnetic field strength at Juno, together with the plasma density model from Voyager 2 entry radio occultation [7], extended to higher altitudes using an exponential fit. Our calculations of the accumulated group delay of field aligned and right-hand polarized waves show a good correspondence to the observed Class 2 whistlers [3]. However, we need to decrease

the overall density profile by a factor of 10 in order to fit the much steeper Class 1 traces.

The propagation delay can also be influenced by properties of the wave mode structure in the extremely low density plasma close to the Juno altitude. In the situation where the plasma frequency becomes comparable to the ion cyclotron frequency, the wave properties drastically change. An example is given in Figure 1, showing the group velocity as a function of frequency and parametrized by the wave vector angle with respect to the local field line. A hook signature on a whistler trace may be generated by a sudden decrease of the group velocity for inclined wave vectors.

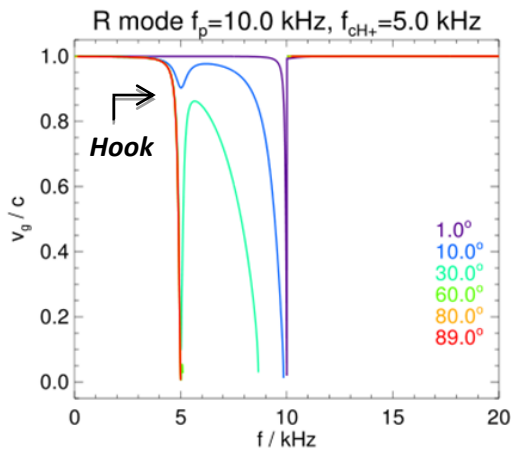


Figure 1: Group velocity of right hand polarized waves for plasma parameters close to Juno orbit.

4. Summary

The Waves instrument onboard Juno collected over sixteen hundred lightning detections, the largest set obtained up to now.

Observed peak occurrence rates of more than 4 whistlers/second in short orbital segments and an average rate of more 1 whistler/second in midlatitudes are similar to thunderstorms at Earth.

Comparison of their frequency-time structure with calculations of their frequency dependent group delay allows us to estimate parameters of the topside ionosphere of Jupiter. Their dispersion properties can be explained by peculiar properties of the mode

structure and group velocity for extremely low plasma densities.

Short duration of Class 2 electron whistlers can be explained by dispersion calculations based on existing models of ionospheric plasma and magnetic field. Even shorter duration of Class 1 whistlers might reflect density holes in the ionosphere, not detected by previous radio occultation measurements. Steep frequency-time signatures of class 1 whistlers in the northern hemisphere indicate that the ionospheric plasma may have different properties in the two hemispheres.

Acknowledgements

The authors would like to acknowledge all members of the Juno mission team, especially the engineers and staff of the Juno Waves instrument. The research at the University of Iowa was supported by NASA through Contract 699041X with the Southwest Research Institute. The work of I.K. and O.S. was supported by the MSM100421701 and LTAUSA 17070 grants and by the Praemium Academiae award.

References

- [1] Gurnett et al. (1979): Whistlers observed by Voyager 1: Detection of lightning on Jupiter. *Geophys. Res. Lett.* 6, 511–514.
- [2] Bolton, et al. (2017): Jupiter’s interior and deep atmosphere: The initial pole-to-pole passes with the Juno spacecraft. *Science* 356, 821–825.
- [3] Kolmašová et al (2018): Discovery of rapid whistlers close to Jupiter giving implying similar lightning rates as at on Earth . *Nature Astronomy* (in the press).
- [4] Kurth et al. (2017): The Juno Waves investigation. *Space Sci Rev.* 213, 347–392, doi:10.1007/s11214-017-0396-y
- [5] Brown et al. (2018): Prevalent lightning sferics at 600 megahertz near Jupiter’s poles. *Nature* (in the press).
- [6] Connerney et al. (1998): New models of Jupiter’s magnetic field constrained by the Io flux tube footprint. *J. Geophys. Res. Sp. Phys.* 103, 11929–11939.
- [7] Hinson et al. (1998): Jupiter’s ionosphere: New results from Voyager 2 radio occultation measurements. *J. Geophys. Res.* 103, 9505–9520.

Long-term behavior of Jovian polar vortices from JunoCam observations

F. Tabataba-Vakili (1), G. S. Orton (1), C. J. Hansen (2), J.H. Rogers (3), G. Eichstädt (4), T.W. Momary (1), M. Caplinger (5), M. Ravine (5), S. Bolton (6).

(1) Jet Propulsion Laboratory, California Institute of Technology, Pasadena, California, USA; (2) Planetary Science Institute, Tucson, Arizona, USA; (3) British Astronomical Association, London, UK; (4) Independent scholar, Stuttgart, Germany; (5) Malin Space Science Systems, San Diego, California, USA; (6) Southwest Research Institute, San Antonio, Texas, USA
 (fachreddin.tabataba-vakili@jpl.nasa.gov)

Abstract

The Juno spacecraft has discovered constellations of circumpolar cyclones about the poles of Jupiter. The shape of these constellations has remained stable over the last 1.5 years of observation. However, an in-depth, long-term analysis of the location and characteristics of the circumpolar cyclones is necessary to compare the observed phenomenon with existing theories.

Introduction

NASA's Juno spacecraft[1] provides unprecedented observations of the polar regions of Jupiter. Observations with the JunoCam[2, 3] and JIRAM instruments [4] on Juno have identified cyclonic vortices around the poles of Jupiter. These circumpolar cyclones (CPCs) have been characterized as mostly stable configurations of eight and five CPCs, respectively spread around the geographical north and south poles, each with a central cyclone located in close proximity to the pole[4].

Measurements of the poles are performed close to the time of closest approach, i.e. perijove (PJ), which occurs roughly every 53 days. JunoCam can be oriented to observe the poles of Jupiter at every of the currently planned perijoves. JunoCam is limited to observing the illuminated day-side of Jupiter, so one PJ observation with JunoCam will only include half of the north polar region and more of the south polar region as it is viewed for longer. These measurements are taken close to the Jovian northern winter solstice so the south pole is better illuminated due to the Jovian axial tilt of 3 degrees.

Circumpolar Cyclones

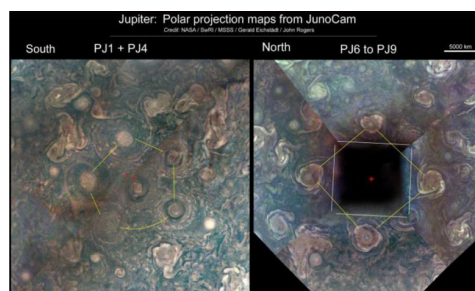


Figure 1: Composite image of perijove observations 1 and 4 of Jupiter's south pole (left) and of perijove observations 6 through 9 of Jupiter's north pole (right). Adapted from [5].

Composite images of JunoCam observations from different perijoves (Figure 1) reveal a pentagonal constellation in the south pole and an octagonal (ditetragonal) constellation in the north pole. Repeated observations show that the overall arrangement of the CPCs seems to be mostly stable and that individual CPCs do not move far from the observed configuration between perijoves.

The constellation of circumpolar cyclones has remained largely constant over the last 1.5 years of observation. Figure 2 exemplifies this by showing the south-polar pentagonal structure of circumpolar cyclones during PJ12.

Vortex Crystals

A current hypothesis is that the eight- and five-sided structures of circumpolar cyclones may be similar to

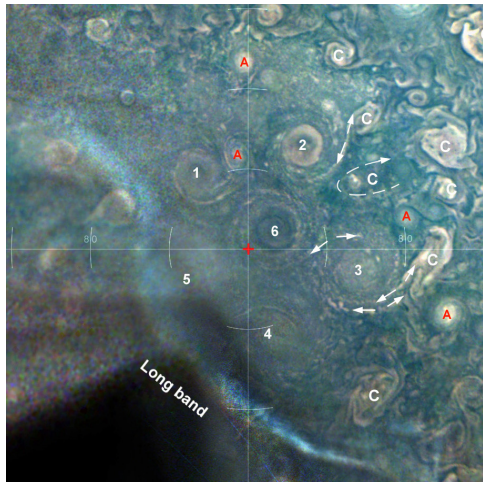


Figure 2: Southern polar region during perijove 12.

so-called vortex crystals[4]. These vortex crystals are characterized by a stable, symmetric configuration of vortices around a circle. Figure 3 shows examples of these configurations that show the most similarity with the observed vortex constellations of Jupiter. Vortex crystals can emerge in inviscid incompressible two-dimensional fluids due to relaxation of a turbulent initial state into a state of maximum entropy[7]. So far, real-life examples of this phenomenon have only been observed in experiments of rotating superfluid helium and Bose-Einstein condensates, as well as magnetized electron columns and super-conductors.

Long-term evolution

To understand the mechanisms behind the stability of the circumpolar cyclones and test how well vortex crystal theory is applicable we need to quantify the long-term behavior of the Jovian circumpolar cyclones. The long-term tracking of cyclone location is especially important for characterizing the stability of their constellation.

For this purpose we aim to use the ISIS3 imaging processing tool to achieve an improved mapping for the JunoCam images.

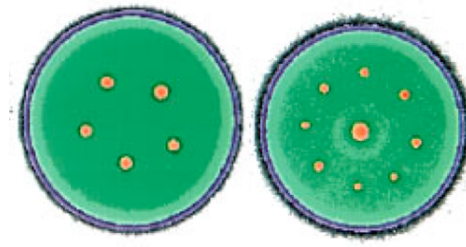


Figure 3: Examples of vortex crystal structures. Adapted from [6].

Acknowledgements

This research was largely funded by NASA through the Juno project. A portion of this was distributed to the Jet Propulsion Laboratory, California Institute of Technology.

References

- [1] Bolton, S. J., the Juno Science Team (2010). "The Juno mission." *Proceedings of the International Astronomical Union*, 6(S269), 92-100.
- [2] Hansen, C. J., et al. "Junocam: Juno's outreach camera." *Space Science Reviews* 213.1-4 (2017): 475-506.
- [3] Orton, G.S., et al. "The first close-up images of Jupiter's polar regions: Results from the Juno mission JunoCam instrument." *Geophysical Research Letters* 44.10 (2017): 4599-4606.
- [4] Adriani, A., et al. "Clusters of cyclones encircling Jupiter's poles." *Nature* 555.7695 (2018): 216-219.
- [5] Rogers, J. H., et al. "Jupiter's polar polygons: Circumpolar clusters of cyclones." *J. Brit. Astron. Assoc.* 128 (2018): 67.
- [6] Schechter, D. A., et al. "Vortex crystals from 2D Euler flow: Experiment and simulation." *Physics of Fluids* 11.4 (1999): 905-914.
- [7] Jin, D. Z., and Daniel HE Dubin. "Regional maximum entropy theory of vortex crystal formation." *Physical Review Letters* 80.20 (1998): 4434.

JunoCam Imaging Jupiter through PJ14

M. A. Ravine (1), C. J. Hansen (2), G. S. Orton (3), C. Thepenier (3), T. W. Momary (3), M. A. Caplinger (1), S. K. Atreya (4), A. P. Ingersoll (5), S. J. Bolton (6), F. Tabataba-Vakili (3), J. H. Rogers (7) and G. Eichstädt (8).

(1) Malin Space Science Systems, San Diego, California, USA (ravine@msss.com), (2) Planetary Science Institute, Tucson, Arizona, USA, (3) Jet Propulsion Laboratory, California Institute of Technology, Pasadena, California, USA, (4) University of Michigan, Ann Arbor, Michigan, USA, (5) Division of Geological and Planetary Sciences, California Institute of Technology, Pasadena, California, USA, (6) Southwest Research Institute, San Antonio, Texas, USA, (7) British Astronomical Association, London, UK and (8) Independent scholar, Stuttgart, Germany.

Abstract

Juno's imaging system, JunoCam, acquired moderate- to high-resolution color images of Jupiter over all latitudes. We have detected a variety of features in these images, for example: long-lived circumpolar cyclones, very small cumulus-like cloud features generically referred to as "pop-up clouds", high-altitude hazes, and an abundance of "mesoscale" wave trains.

1. Introduction

Juno's imaging system, JunoCam, has acquired color images of Jupiter for thirteen of the first fourteen perijove passes (PJ1 through PJ14, but not PJ2). The moderate-resolution polar images and high-resolution images at lower latitudes show an atmospheric circulation much more complex than previously detected.

2. JunoCam Instrument

JunoCam has a single CCD detector with an integral color-strip filter that enables the instrument to image in four color bands—blue, green, red and the 889-nm methane band. The JunoCam lens maps a field of view of 58° across the width of the detector, perpendicular to the spacecraft scan direction. Repeated readout of the filtered sections of the CCD with rotation allows JunoCam to build up a color image. While the nominal design life of the camera was eight perijove passes, it continues to function after fourteen passes with no radiation-induced degradation. For details, see Hansen et al. (1).

3. JunoCam Imaging

Around each perijove pass of the Juno spacecraft, JunoCam acquires multiple half-disk color images of

the North and South Poles at high emission angle ($> 70^\circ$). These images have a spatial scale at the cloud tops of ~ 50 km/pixel. Resolution increases at lower altitudes and latitudes, to a minimum of less than 5 km/pixel at perijove.

3.1 Circumpolar Cyclones

Circumpolar cyclones continue to be static in System III and have not changed their fundamental configuration (**Figure 1**), with eight around the north polar and five around the south pole (2). They rotate cyclonically with velocity increasing with radius from the center. Their centers are generally unmoving or in one case, actually anticyclonic.

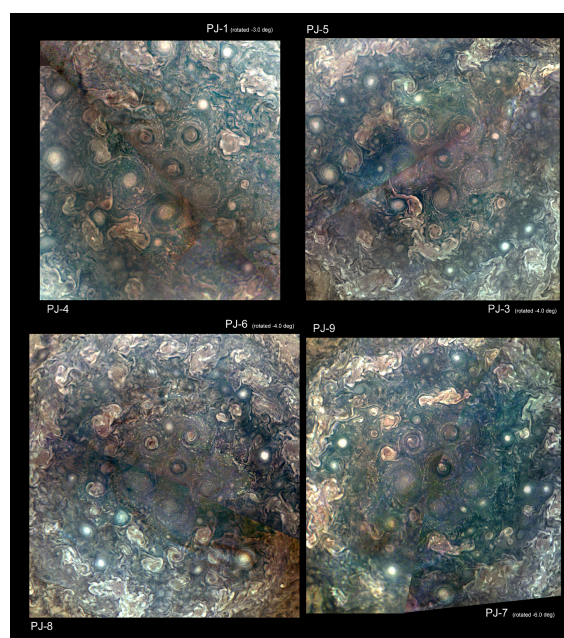


Figure 1: Southern Circumpolar Cyclones have been stable in System III for more than one year.

3.2 “Pop-up” Clouds

These are detected in several regions identified with upwelling, usually bright clouds (**Figure 2**), as well as with brighter banded features within the Great Red Spot. They are on the order of 50 km or smaller – down to the resolution limit of the instrument, often with shadows around the same size.



Figure 2: “Pop-up” clouds in the South Temperate Zone, PJ6.

3.3 Mesoscale Waves

We have detected numerous instances of wave trains with wavelengths mostly smaller than those of the mesoscale gravity waves detected by Voyager, Galileo, New Horizons and the Hubble Space Telescope. They are on the same size of the shortest wavelengths detected by the Voyager-2 imaging system. Their wavelengths lie within the 70 - 190 km range (**Figure 3**). Excepting one occurrence at the northern margin of the Great Red Spot, all were found with 10° latitude of the equator. Because of the constrained time sampling dictated by Juno’s orbit, it is not possible to estimate the phase velocity of these wave, placing limitations on assessment of alternative mechanisms for their origin.

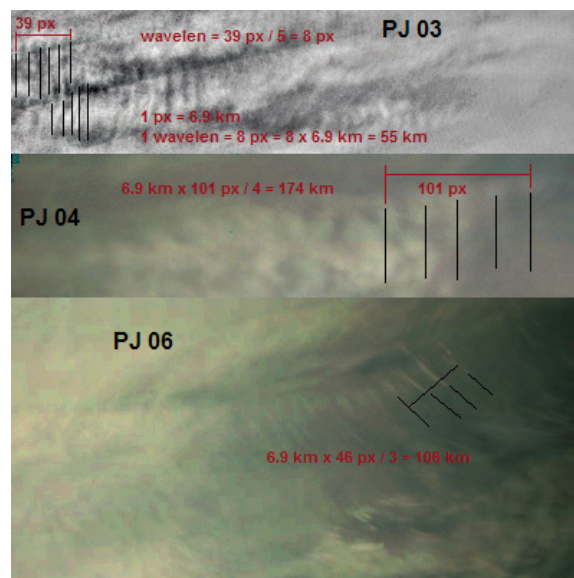


Figure 3: Examples of mesoscale waves.

4. Summary and Conclusions

JunoCam has acquired observations of Jupiter on fourteen successive Juno orbits, revealing a diversity of atmospheric features not previously observed. Orton et al. (3) provide a more detailed discussion of the polar features, as observed in Juno’s first perijove. JunoCam will continue these observations for the rest of the Juno Mission.

Acknowledgements

This research was funded by the National Aeronautics and Space Administration through the Juno Project. A portion of these funds were distributed to the Jet Propulsion Laboratory, California Institute of Technology. All JunoCam images can be obtained on the Mission Juno web site (<https://www.missionjuno.swri.edu>).

References

- [1] Hansen, C. J., et al. JunoCam: Juno’s outreach camera. Space Sci. Rev. 2014. doi10.007/s/11214-014-0079-x
- [2] Adriani et al. Clusters of cyclones encircling Jupiter’s poles. Nature. 555, 216-219. 2018. doi 10.1038/nature25491.
- [3] Orton, G. S, et al. The first close-up images of Jupiter’s polar regions: Results from the Juno mission JunoCam instrument. Geophys. Res. Lett. 44, 2017. doi: 10.1002/2016GL072443.

Juno's sensitivity to the gravitational signature of Jupiter's meridional flows

D. Durante (1), V. Notaro (1), P. Racioppa (1), E. Galanti (2), Y. Kaspi (2), and L. Iess (1)

- (1) Sapienza University of Rome, Department of Mechanical and Aerospace Engineering, Rome, Italy
(daniele.durante@uniroma1.it)
(2) Department of Earth and Planetary Sciences, Weizmann Institute of Science, Rehovot, Israel

Abstract

The Juno spacecraft is currently orbiting Jupiter in a highly-eccentric, 52.9-day orbit, unveiling the interior structure of the gas giant. Since its arrival in Jupiter's system on July 4th, 2016, Juno has completed several revolutions about the planet (15 pericenter passes as of September 2018), revealing fundamental details of Jupiter's interior structure and atmospheric dynamics.

Juno's radio science experiment provides an extremely accurate determination of Jupiter's gravity field, to an unprecedented level of detail. During gravity-dedicated pericenter passes, Juno establishes a two-way coherent radio link with NASA's Deep Space Network DSS 25 antenna, located in Goldstone's desert, which acquires Doppler measurements at Ka and X bands (32.5 and 8.4 GHz). The two simultaneous radio links enable an incomplete calibration of dispersive noise (up to 75%), mainly induced by solar corona (especially important when the signal passes close to the Sun) and by the Io plasma torus (the signal passes through the torus at every pericenter pass, due to orbital geometry). Earth's tropospheric noise is strongly reduced using the Advanced Media Calibration System, which measures the path delay variations caused by tropospheric water vapor. The resulting end-to-end range rate noise is about 0.015 mm/s at 60 s integration time, therefore enabling a very accurate determination of Jupiter's gravity field.

The data acquired through Juno's state-of-the-art radio system from the first two gravity passes, PJ3 and PJ6, were combined in a multi-arc solution to estimate the zonal coefficients of the spherical harmonic expansion of Jupiter's gravity field [1]. The comparison of the observed even and odd zonal

the surface zonal winds extend to a depth of thousands of kilometers [2, 3].

The zonal jets produce a very strong gravitational signal that has been observed for the very first time. In addition, local features at Jupiter's cloud level produce tiny signals that may be detected by Juno's radio system [4]. In principle, these structures may have an e-folding depth which differs from that of the main zonal flows. By the end of the mission (30 July 2021), Juno will complete a total of 25 gravity-dedicated orbits, providing a uniform coverage in longitude of Jupiter's gravitational field. It will be possible to exploit the full data set to determine if any non-zonal component of the gravity field is present and eventually relate it to the gravitational signature of Jupiter's meridional flows. The magnitude of the non-zonal component of the gravity field provides information on the depth of the non-zonal atmospheric circulation, i.e., the meridional flows.

We report on a preliminary analysis of the available data set, which already excludes the case in which meridional flows penetrate as deep as, or deeper than, the zonal flows, according to theoretical predictions. In addition, we report on numerical simulations of the gravity experiment and discuss the expected results at the end of the mission.

Acknowledgements

This research was carried out under the sponsorship of the Italian Space Agency and the Israeli Space Agency.

References

- [1] Iess, L., W. M. Folkner, D. Durante, M. Parisi, Y. Kaspi, E. Galanti, T. Guillot, W. B. Hubbard, D.J.

Milani, R. Park, P. Racioppa, D. Serra, P. Tortora, M. Zannoni, H. Cao, R. Helled, J.I. Lunine, Y. Miguel, B. Militzer, S. Wahl, J.E.P. Connerney, S.M. Levin, S. J. Bolton (2018). *The measurement of Jupiter's asymmetric gravity field*, Nature 555, pp. 220-222.

[2] Kaspi, Y., E. Galanti, W. B. Hubbard, D. J. Stevenson, L. Iess, T. Guillot, J. Bloxham, H. Cao, D. Durante, W. Folkner, R. Helled, A. P. Ingersoll, J. I. Lunine, Y. Miguel, B. Militzer, M. Parisi, S.M. Wahl, J. E. P. Connerney, S. M. Levin, and S. J. Bolton (2018). *The extension of Jupiter's jet to a depth of thousands of kilometers*, Nature 555, 223-226

[3] Guillot, T., Y. Miguel, B. Militzer, W.B. Hubbard, E. Galanti, Y. Kaspi, H. Cao, S. Wahl, L. Iess, W.M. Folkner, R. Helled, D.J. Stevenson, J.I. Lunine, D. Reese, A. Biekman, M. Parisi, D. Durante, J.E.P. Connerney, S.M. Levin, S. J. Bolton (2018). *A suppression of differential rotation in Jupiter's deep interior*, Nature 555, 227-230.

[4] Parisi, M., E. Galanti, S. Finocchiaro, L. Iess, and Y. Kaspi (2016). *Probing the depth of Jupiter's Great Red Spot with the Juno gravity experiment*, Icarus 267, 232-242.

Toward modeling Jupiter's 3D shape and gravity field

Nadine Nettelmann
 Institut für Physik, Universität Rostock, Germany (nadine.nettelmann@uni-rostock.de)

Abstract

We present our preliminary results for the static tidal response of Jupiter and Saturn to the gravitational field perturbations raised by their satellites. Assuming a constant density interior, we find the fluid Love number k_2 of rotationally flattened planet models to be strongly enhanced compared to non-rotating planet models. Assuming a polytropic equation of state, this effect reduces by about a factor of two. We compare our predictions to recent measurements of k_2 based on Cassini data for Saturn and Juno data for Jupiter.

1. Introduction

The gas giant planets in the outer solar system, Jupiter and Saturn, are rapid rotators. They experience strong rotational flattening, which can be seen from their oblate shapes. Accordingly, also their gravity fields are non-spherical. Several gravitational moments have recently been accurately measured by the Cassini spacecraft at Saturn and the Juno spacecraft at Jupiter, respectively.

Deviations in shape and gravity field from perfect spherical symmetry allow us to look into the planetary deep interior, as the strength of deviation depends on internal mass density distribution. The latter in turn is influenced by composition (typically distinguished into hydrogen, helium, and heavy elements), composition distribution (e.g., the size of a core or the atmospheric metallicity), and the equations of state. For gas giant planets like Jupiter, the hydrogen equation of state matters most. Indeed, uncertainties in the behavior of hydrogen and helium under planetary interior conditions still lead to significant uncertainties in our understanding of internal structure and evolution. For instance, cool and dense Jupiter adiabats tend to predict sub-solar atmospheric metallicity, while warmer Jupiter adiabats yield heavy element-rich deep envelopes [4].

2. Tidal perturbation

Conventional Jupiter models assume symmetry of the mass density around the axis of rotation. This case applies to isolated fluid planets in hydrostatic equilibrium with spin axis perfectly aligned with the principal axis of inertia, and no winds. Jupiter and Saturn however are surrounded by satellites. The gravity field of a satellite can raise tides that break the symmetry. Moreover, zonal flows observed on Jupiter may also give rise to a longitudinal variation [1]. The longitudinal contribution can be expressed in terms of so-called tesseral moments C_{nm} and S_{nm} . Indeed, Juno measurements indicate non-zero moments C_{21} and S_{21} , while for the C_{22} and S_{22} components upper limits could already be inferred [1]. The uncertainty will decrease in the further course of the Juno mission as Juno is going to take a full 3D map of Jupiter's gravity field.

Assuming a single tide-raising perturber, the tesseral moments can be translated into the Love numbers k_{nm} according to [6]

$$k_{nm} = -\frac{3}{2} \frac{(n+m)!}{(n-m)!} \frac{C_{nm}}{P_n^m(0)q_{\text{tid}}} (r_S/R)^{2-n}, \quad (1)$$

where r_S is the planet-satellite distance, R is planet radius, and q_{tid} is the tidal forcing. For strong rotational forcing, the Love numbers k_{nm} are splitted and deviate from that of a spherical body.

Figure 1 shows current measured Love number k_{22} values of Jupiter from the Juno mission [1] and of Saturn including Cassini data [3] as well as theoretical predictions. Models that assume a spherical shape (e.g., [3], the yellow-black-dotted model by [6] for Saturn, and [5]), yield k_{22} values lower than the measured ones. In contrast, the yellow-black-dashed model [6] takes into account the rotational flattening in the tidal response calculation. This leads to $\sim 12\%$ stronger response; it clearly appears to be required to explain Jupiter's observed value.

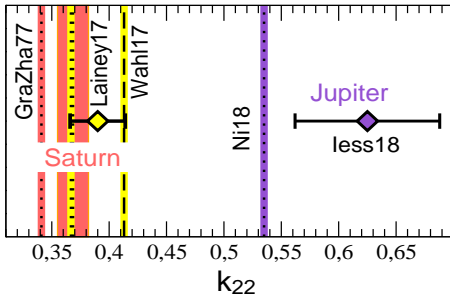


Figure 1: Static Love number k_{22} values of Jupiter (violet), Saturn (yellow, red) from Juno [1] and Cassini [3] observations (diamonds with error bars), and from planet models. Dotted lines: for spherical shape [3, 6, 5], dashed line: for rotationally flattened shape [6].

3. Preliminary results

Figure 2 shows preliminary results of this work for the tidal response of rotationally flattened Jupiter and Saturn assuming a simplified constant-density interior. The models were calculated following the method of [6]. For the Jupiter-Io and the Saturn-Tethys system we find, respectively, a strong 20% and 30% enhancement in the Love number k_{22} value due to the rotational flattening compared to the analytically known value for a spherical fluid planet, $k_2 = 1.5$. More centrally condensed models that are constrained by the low-order gravitational harmonics are expected to yield a less pronounced tidal response.

4. Outlook

Further work will address the influence of various effects on the static fluid Love number k_{nm} values of Jupiter. In particular, we will apply different physical equations of state, take into account mis-aligned rotation and principal axes, and a possible phase lag of the tidal bulge. The resulting predictions for an otherwise rigidly rotating Jupiter will help to disentangle the influence of winds, and thus provide and additional constraint on Jupiter's dynamic atmosphere.

As has been shown for Saturn [2, 6], different interior models which match the low-order gravitational harmonics yield extremely similar k_{22} values. Therefore, any offset between the measured and the predicted value will yield unique hints on missing physical effects in the tidal response calculation. Thanks to

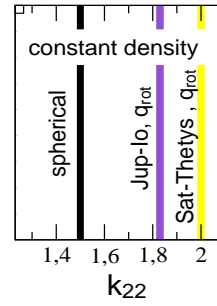


Figure 2: Same as Figure 1 but for constant density models and spherical shape (black), or Jupiter's and Saturn's rotational forcing.

the current space-based Juno measurement of Jupiter's gravity field, this opens the opportunity of a new era of interior modeling.

Acknowledgements

This work is supported by the German Science Foundation under DFG grant NN1734/1.

References

- [1] Iess L., W.M. Folkner, D. Durante, et al.: Measurement of Jupiter's asymmetric gravity field, *Nature*, vol. 555, 220, 2018.
- [2] Kramm U., Nettelmann N., Redmer R., Stevenson D.S.: On the degeneracy of the tidal Love number k_2 in multi-layer planetary models, *A&A*, vol. 528, A18, 2011.
- [3] Lainey, V. R.A. Jacobson, R. Tajeddine, et al.: New constraints on Saturn's interior from Cassini astrometric data, *Icarus*, vol. 281, 286, 2017.
- [4] Miguel Y., Guillot T., Fayon I.: Jupiter internal structure: effect of different EOS, *A&A*, vol. 596, A114, 2016.
- [5] Ni, D.: Moment of inertia and tidal Love number k_2 , *A&A*, DOI 10.1051/0004-6361/201732183, 2018.
- [6] Wahl S., W.B. Hubbard, B. Militzer: The CMS method with tides and a rotational enhancement of Saturn's tidal response, *Icarus*, vol. 282, 183, 2017.

A possible determination of Jupiter's frequency-dependent tides at the end of the Juno mission

Virginia Notaro, Daniele Durante and Luciano Iess

Department of Mechanical and Aerospace Engineering, Sapienza University of Rome, Rome, Italy
(virginia.notaro@uniroma1.it)

Abstract

Juno has currently completed 12 orbits around Jupiter, of which 5 have been dedicated to the gravity science experiment. The gravity experiment consists in the measurement of the Doppler shift of X- and Ka- band signals transmitted from NASA's DSS 25 antenna to the spacecraft and retransmitted back coherently to the same station (two-way link). The Doppler data are used to accurately reconstruct the trajectory of the spacecraft, whilst determining several geophysical parameters (such as the harmonic coefficients of Jupiter's gravity field) to characterize the gas giant's interior mass distribution [1].

The analysis of Doppler data from the Juno spacecraft allowed to determine Jupiter's gravity field with unprecedented accuracy, as well as to reveal the depth of its atmospheric zonal winds [2, 3].

Until the end of the nominal mission in July 2021, Juno will complete 20 additional gravity orbits. The full dataset will be fundamental to uncover features of Jupiter's gravity not currently observable, such as the planet's response to the frequency-dependent tides raised by the satellites as they orbit around the planet with different periods.

[4] computed Jupiter's static Love numbers (the geophysical parameters that characterize a planet's response to a tidal perturbation) for Io, Europa and Ganymede, the main tide-raising bodies for the gas giant. In addition, resonances between the frequencies of the tidal perturbation and Jupiter's natural oscillation eigenfrequencies, not considered in their paper, could amplify the dynamical response of the planet to the satellite-dependent perturbation.

Nevertheless, no theory can currently predict the dynamical tidal response of Jupiter to tides raised by its moons. [5] developed an incomplete dynamical theory by computing the frequency-dependent Love numbers as a function of the satellite mean motion and

of Jupiter's oscillation eigenfrequencies. However, they did not consider the fast rotation of the gas giant, which increases its tidal response [6].

We report on simulations performed over the nominal science mission to determine whether Juno is sensitive to frequency-dependent tides on Jupiter. In fact, Doppler measurements from the Juno spacecraft can be used to sample the tidal bulge raised on Jupiter by its moons. We first simulated Doppler data from Juno considering a 6-hour two-way link from NASA's DSS 25 antenna at X- and Ka-band, covering the pericenter, along with an additional 3-hour X-band two-way tracking window from NASA DSS 43. We assumed a realistic noise level on the Doppler observables (1.4 mHz for Ka-band and 0.6 mHz for X-band at 60-s integration time), coherently with the results from data analysis [2].

For the parameter estimation, we used a multi-arc least-square batch filter that provides an estimate of the solve-for parameters by minimizing the difference between the simulated measurements and the ones computed with a dynamical model of the spacecraft. The solve-for vector is divided into local parameters, which pertain to each gravity pass (such as the spacecraft's state), and global parameters. The tidal model currently used for gravity data analysis assumes that the Jovian satellites contribute equally to the total tidal perturbation, and thus only one Love number is estimated. We implemented a frequency-dependent tidal model within the orbit determination software, defining one Love number for each of the Galilean satellites.

We defined as global parameters Jupiter's GM and its gravity field up to zonal degree 30 and tesseral order 4, as well as the frequency-dependent Love numbers for Io, Europa, Ganymede and Callisto up to degree and order 4. We also included the motion of Jupiter's spin-axis (pole position and rate), and we considered the uncertainty on the GM of the Galilean

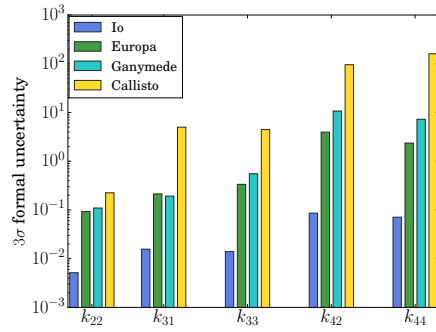


Figure 1: 3σ formal uncertainty on the Love numbers up to degree and order 4 for Io (blue), Europa (green), Ganymede (cyan) and Callisto (yellow).

satellites to account for errors in their trajectories.

The formal uncertainty obtained on the satellite-dependent Love numbers after the nominal 25 gravity-dedicated orbits is shown in Figure 1. Juno shows good sensitivity to tides raised by Io, Europa and Ganymede, the main sources of the tidal perturbation. The uncertainty on the Love numbers for a given degree and order increases with the distance from the planet, and grows also with increasing degree of the perturbation.

The results of our simulations show that Juno is indeed sensitive to frequency-dependent tides on Jupiter. However, a future determination of this effect, and thus a separation of the different contributions, depends on the actual values of the satellite-dependent Love numbers, which cannot be currently predicted in the framework of the dynamical tidal response. The determination of frequency-dependent tides with Juno would shed further light on Jupiter’s interior mass distribution and stratification, and would contribute to the development of a new theory for dynamical tides on fast-rotating giant planets.

Acknowledgements

This work has been carried out under sponsorship from the Italian Space Agency.

References

- [1] Asmar, S.W., Armstrong, J.W., Iess, L., Tortora, P.: Spacecraft Doppler tracking: noise budget and accuracy achievable in precision radio science observations, *Radio Science*, Vol. 40, 2005.
- [2] Iess, L., Folkner, W.M., Durante, D., Parisi, M., Kaspi, Y., Galanti, E., Guillot, T., Hubbard, W.B., Stevenson, D.J., Anderson, J.D., Buccino, D.R., Gomez Casajus, L., Milani, A., Park, R., Racioppa, P., Serra, D., Tortora, P., Zannoni, M., Cao, H., Helled, R., Lunine, J.I., Miguel, Y., Militzer, B., Wahl, S.M., Connerney, J.E.P., Levin, S.M., Bolton, S.J.: Measurement of Jupiter’s asymmetric gravity field, *Nature*, Vol. 555, pp. 220-222, 2018.
- [3] Kaspi, Y., Galanti, E., Hubbard, W.B., Stevenson, D.J., Bolton, S.J., Iess, L., Guillot, T., Bloxham, J., Connerney, J.E.P., Cao, H., Durante, D., Folkner, W.M., Helled, R., Ingersoll, A.P., Levin, S.M., Lunine, J.I., Miguel, Y., Militzer, B., Parisi, M., Wahl, S.M.: Jupiter’s atmospheric jet streams extend thousands of kilometres deep, *Nature*, Vol. 555, pp. 223-226, 2018.
- [4] Wahl, S.M., Hubbard, W.B., Militzer, B.: Tidal response of a preliminary Jupiter model, *The Astrophysical Journal*, Vol. 831, 2016.
- [5] Vorontsov, S.V., Gavrilov, S.V., Zharkov, V.N., Leontev, V.V.: Dynamical theory of tides on the giant planets, *Astronomicheskii Vestnik*, Vol. 18, pp. 8-18, 1984.
- [6] Wahl, S.M., Hubbard, W.B., Militzer, B.: The Concentric MacLaurin Spheroid method with tides and a rotational enhancement of Saturn’s tidal response, *Icarus*, Vol. 282, pp. 183-194, 2017.

Assessing quasi-periodicities in Jovian X-ray emissions: techniques and statistical survey of Chandra observations

Jackman, Caitriona (1), Knigge, Christian (1), Altamirano, Diego (1), Gladstone, Randy (2), Dunn, William (3,4), Elsner, Ron (5), Kraft, Ralph (6), Branduardi-Raymont, Graziella (3), Ford, Peter (7)

(1) Department of Physics and Astronomy, University of Southampton, Southampton, SO17 1BJ, UK, (2) Space Science & Engineering Division, Southwest Research Institute, San Antonio, Texas, USA, (3) Mullard Space Science Laboratory, Department of Space & Climate Physics, University College London, Holmbury St. Mary, Dorking, Surrey RH5 6NT, UK, (4) The Centre for Planetary Science at UCL/Birkbeck, Gower Street, London, WC1E 6BT, UK, (5) Harvard-Smithsonian Center for Astrophysics, Smithsonian Astrophysical Observatory, Cambridge, Massachusetts, USA, (6) NASA Marshall Space Flight Center, USA, (7) Kavli Institute for Astrophysics and Space Research, MIT, Cambridge MA, USA (c.jackman@soton.ac.uk)

Abstract

We are currently in an exciting era for jovian science with the Juno spacecraft in orbit around Jupiter and several Earth-based and space-based observatories studying Jupiter's auroral regions in multiple wavelengths. We have more data than ever before, long observing windows (up to 72 ks for Chandra, 144 ks for XMM, and 100 ks for NuStar), and successive observations relatively closely spaced in time. These features combine to allow us to pursue advanced methods for examining quasi-periodicities in the X-ray emission. Previous works have reported individual observations of significant quasi-periodicities emerging from the jovian system in X-ray, UV and radio wavelengths.

We present robust methods for significance testing of emerging quasi-periodicities, searching for coherence in X-ray pulsing over weeks and months, and seeking to understand the robustness and regularity of previously reported quasi-periodic emissions.

Our analysis incorporates the use of the Rayleigh test as an alternative to Lomb-Scargle analysis, where Rayleigh is particularly suited to a time-tagged dataset of spare counts such as is common for jovian X-ray data. Furthermore, the analysis techniques that we present (including Rayleigh and Monte-Carlo simulation) can be applied to any time-tagged dataset (including those from other wavelengths such as UV).

These techniques are applied to a range of Chandra observations from the pre-Juno era (1990s to 2015) and to several Chandra observations taken while Cassini was upstream and at apoJove.

Discovering Jupiter's interior with Juno

Yamila Miguel (1), Tristan Guillot (2) and the Interiors Working Group of Juno Mission
(1)Leiden Observatory, Netherlands (2)Observatoire de la Cote d'Azur, France (ymiguel@strw.leidenuniv.nl)

Abstract

The process of satellite formation is directly linked to the formation of the giant planet that host them. In particular, the formation of Galilean satellites is still not fully understood [1] and therefore a deeper understanding of Jupiter's formation is needed.

In orbit since July 2016, Juno mission had led to a remarkable improving of Jupiter gravity data [2, 3, 4], changing our knowledge of the planetary interior and leading to a much better comprehension of the big giant and its role in the solar system [5, 6, 7].

We use this outstanding gravity data to perform models of Jupiter's internal structure and test different parameters to get a better understanding of Jupiter's interior, including an estimation of the extent of the differential rotation in the deep atmosphere, a long standing question in planetary science and highly relevant to reach a deeper knowledge of Jupiter's internal structure.

References

- [1] Miguel, Y. and Ida, S.: A semi-analytical model for exploring Galilean satellites formation from a massive disk, *Icarus*, Vol. 266, pp. 1-14, 2016.
- [2] Bolton, S., et al.: Jupiter's interior and deep atmosphere: The initial pole-to-pole passes with the Juno spacecraft, *Science*, Vol. 356, pp. 821-825, 2017.
- [3] Folkner, W. M. et al.: Jupiter gravity field estimated from the first two Juno orbits, *Geophys. Res. Lett.*, Vol 44, 4694-4700, 2017.
- [4] Iess, L. et al.: Measurement of Jupiter's asymmetric gravity field, *Nature*, Vol 555, pp. 220-222, 2018.
- [5] Wahl, S. M. et al.: Comparing Jupiter interior structure models to Juno gravity measurements and the role of an expanded core: *Geophys. Res. Lett.*, Vol 44, pp. 4649-4659, 2017.

[6] Guillot, T., Miguel, Y., et al.: A suppression of differential rotation in Jupiter's deep interior, *Nature*, Vol 555, pp. 227-230, 2018.

[7] Kaspi, Y. et al.: Jupiter's atmospheric jet streams extend thousands of kilometres deep, *Nature*, Vol 555, pp. 223-226, 2018.